Journal of Clinical Monitoring and Computing
https://doi.org/10.1007/s10877-024-01250-2

REVIEW

Electroencephalogram monitoring during anesthesia and critical care: a guide for the clinician

Nitin Manohara[1] · Alessandra Ferrari[2] · Adam Greenblatt[3] · Andrea Berardino[4] · Cristina Peixoto[5] · Flávia Duarte[6] · Zahra Moyiaeri[1] · Chiara Robba[7] · Fabio Nascimento[3] · Matthias Kreuzer[8] · Susana Vacas[9] · Francisco A. Lobo[1]

Received: 21 October 2024 / Accepted: 5 December 2024
© The Author(s), under exclusive licence to Springer Nature B.V. 2024

Abstract
Perioperative anesthetic, surgical and critical careinterventions can affect brain physiology and overall brain health. The clinical utility of electroencephalogram (EEG) monitoring in anesthesia and intensive care settings is multifaceted, offering critical insights into the level of consciousness and depth of anesthesia, facilitating the titration of anesthetic doses, and enabling the detection of ischemic events and epileptic activity. Additionally, EEG monitoring can aid in predicting perioperative neurocognitive disorders, assessing the impact of systemic insults on cerebral function, and informing neuroprognostication. This review provides a comprehensive overview of the fundamental principles of electroencephalography, including the foundations of processed and quantitative electroencephalography. It further explores the characteristic EEG signatures associated wtih anesthetic drugs, the interpretation of the EEG data during anesthesia, and the broader clinical benefits and applications of EEG monitoring in both anesthetic practice and intensive care environments.

Keywords Electroencephalogram · Processed electroencephalogram · Anesthetic drugs and EEG signatures · Anesthesia · Depth of anesthesia · Intensive care

1 Introduction

The state of general anesthesia is defined as a reversible drug-induced state of unconsciousness, absence implicit and explicit memory formation, an optimal balance between nociception and antinociception, and the supression of movement and reflexes [1]. in contrast, other sedative states involve lighter planes of altered arousal with a relative balance between antinociception and paralysis [2]. These altered states of arousal result from profound changes in the central nervous system physiology, induced by varying combinations of hypnotic and antinociceptive drugs, each targetting different neuronal circuits through distinct mechanisms [2, 3]. These changes include loss of cortico-cortical and thalamo-cortical functional connectivity [4], disruption of anticorrelation between the default- and executive-control systems [5], and impaired connectivity between the thalamus and brain stem [6].

Paradoxically, despite the significant effects anesthetic drugs have on multiple neural networks, anesthesiologists have traditionally adhered to the "Leonardo Da Vinci anesthetic paradigm" [7]: *tears come from the heart and not from*

✉ Francisco A. Lobo
francisco.lobo@me.com

1 Division of Anesthesiology, Cleveland Clinic Abu Dhabi, Integrated Hospital Care Institute, Abu Dhabi, United Arab Emirates

2 RCCS Policlinico San Martino, Genoa, Italy

3 Department of Neurology, Washington University in St Louis, St Louis, MO, USA

4 Department of Surgical Sciences and Integrated Diagnostics, University of Genoa, Genoa, Italy

5 Department of Anesthesiology, ULSTMAD, Vila Real, Portugal

6 Department of Anesthesiology, Hospital Garcia de Orta, Almada, Portugal

7 IRCCS Policlinico San Martino, Genoa, Italy

8 Department of Anesthesiology and Intensive Care Medicine, School of Medicine and Health, Technical University of Munich, Munich, Germany

9 Department of Anesthesia, Critical Care and Pain Medicine, Massachusetts General Hospital, Harvard Medical School, Boston, MA, USA

Published online: 20 December 2024

SHOUT
SHARE
IT

the brain [8]. Clinicians use surrogate parameters such as blood pressure or heart rate variation to assess the adequacy of anesthesia instead of directly monitoring the brain, the main target for anesthetic drugs.

Catastrophic events like intraoperative awareness [9], triggered the development of monitors processing the frontal electroencephalographic signal [10] yielding a numerical dimensionless scale of alertness [11], a very simplified approach to monitoring brain activity during anesthesia. The launch of the Bispectral Index (BIS®) (Medtronic, Dublin, Ireland) monitor opened a promising window into the brain and increased the interest of anesthesiologists in perioperative brain monitoring. During the last 30 years, with the introduction of many other monitors with the capacity to process the electroencephalogram (EEG) and derive similar dimensionless scales, applied electroencephalography in anesthesiology and critical care moved from focusing on intraoperative awareness prevention to a broader range of indications with attention turned towards a better comprehension of the raw EEG signal, spectral analysis and different signatures of anesthetic drugs [12, 13]. After two decades of extensive clinical research investigating the basic neurobiological foundations for the use of EEG during anesthesia and intensive care using processed EEG (pEEG) [14–24], we have landed on a curious and paradoxical situation: while there is a general agreement that EEG (processed, quantitative, and/or raw signals) should be used, several surveys and audits still show underuse of such monitoring [25–28].

The I-PROTECT group published a consensus document in this Journal [29], defining and clarifying the key parameters of non-invasive brain monitoring technologies. Building on that foundational report, we aimed to provide a comprehensive review bridging the gap between theoretical framework and the clinical implementation and use of perioperative EEG. This review covers the basic principles of electroencephalography, the tenets of processed and quantitative electroencephalography, the characteristic EEG signatures of anesthetic drugs, the interpretation of the EEG during anesthesia, and the overall benefits of EEG monitoring during anesthesia and intensive care. We also highlight respective limitations, sharing examples of how applied electroencephalography can be integrated into a broader multimodal monitoring strategy to optimize care.

1.1 Part I: foundations of electroencephalography

The EEG signal is a graphical representation recorded at the scalp's surfaceof the measured voltage at a given point in space as compared with a reference value and plotted over time. The measured signal reflects fluctuations in local field potentials generated by the spatiotemporal summation of excitatory and inhibitory postsynaptic potentials in the extracellular milieu and arises primarily as an effect of synchronous activity in cortical pyramidal neurons in layers III, V, and VI [30]. In addition, the EEG signal exhibits minor contributions from non-synaptic intercellular activity, neuron-glial interactions, and subcortical inputs from the dorsal thalamus.

The EEG signal may arise from sources within the brain (true EEG) or sources outside the brain (artifact) which may result from physiologic or environmental generators [31]. Fundamentally, this signal is a collection of superimposed waveforms that can be mathematically deconstructed into constituent frequencies modeled by simple harmonic oscillators. Whereas an oscillation refers to a periodic, regular variation of a parameter as it is displaced around a central value, a waveform is the 2-dimensional graphical representation of an oscillation as it moves through space or time [32]. A wave refers to the shape or morphology of a single cycle within a waveform.

An EEG waveform, like every waveform, has four defining properties:

1. Frequency, f, measured in Hertz (Hz) and is the number of wave repetitions per second.
2. Phase, ϕ, indicates where the wave is in its cycle; it is measured in degrees ($0°-360°$) or radians ($0–2\pi$); for example, it is possible to phase shift a wave backward and forward in time.
3. Amplitude, A, defined as the peak to through distance, representing the voltage and measured in microvolts (μV).
4. Power, P, the square of the amplitude and represents the energy over time.

Scalp EEG is classically divided into five frequency bands; however, only four bands are typically appreciated on surface EEG. Resistance imposed by the skull and soft tissue normally filters out gamma activity (Fig. 1 and 2) [33]:

- Delta, < 4 Hz;
- Theta, 4—< 8 Hz;
- Alpha, 8—< 13 Hz;
- Beta, 14—< 30 Hz.

"Rhythm" refers to EEG activity consisting of monomorphic waves of approximately constant periods with an absence of disruption between wave cycles. For example, the posterior dominant rhythm (PDR) seen during relaxed wakefulness is distributed maximally over the posterior regions of the head, while the Mu rhythm, maximal over the central or centro-parietal regions during relaxed wakefulness, is composed of arc-shaped waves predominantly within the

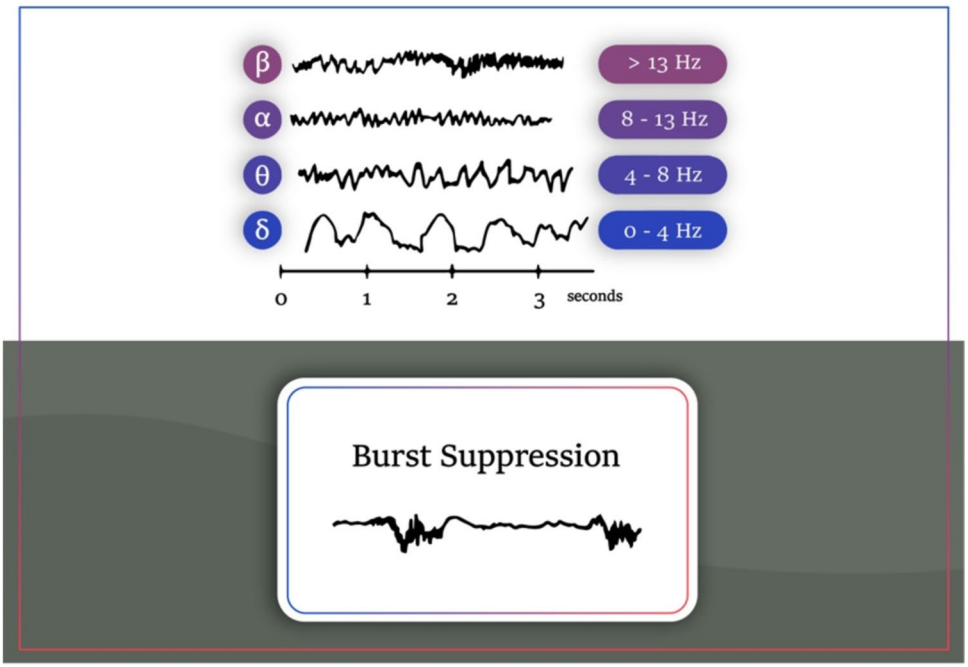

Fig. 1 Various waveform frequencies encountered in the electroencephalogram and the abnormal pattern of burst suppression

alpha band and can be attenuated by the thought of moving the contralateral limb.

1.1.1 Alpha (α) activity

Alpha waves are waves with a duration of 1/8 −1/13 s (77–125 ms) and are the component of the alpha rhythm. As mentioned above, the posterior dominant rhythm is an alpha rhythm occurring at 8- < 13 Hz during relaxed wakefulness over the posterior regions of the head, generally with maximum amplitudes over the occipital areas. It attenuates or disappears with drowsiness, concentration, stimulation, or visual fixation. [33, 35, 36]

1.1.2 Spindles

Spindles are rhythmic oscillations characterized by a waxing and waning shape, progressively increasing, then gradually decreasing, in amplitude (Fig. 3). The sleep spindles constitute a train of distinct waves, usually with a frequency between 12 and 14 Hz and a duration from 0.5 to several seconds, occurring during stage II non-REM (NREM) sleep. Spindle oscillations are fundamentally of thalamic origin, reflecting activity intrinsic to thalamo-cortical connections, and appear from the extensive hyperpolarization of thalamic neurons [37]. Interestingly, spindle-like waveforms may be seen during anesthesia with propofol [38], reflecting cortico-thalamic hypersynchrony induced by this drug [39, 40]. However, spindles induced by propofol occur as a sequence of two or three waxing and waning oscillations, with a break separating an asymmetric waveform underlain by a slow wave [41] and distinct from those generated by low doses of dexmedetomidine [42–46].

1.1.3 Beta (β) activity

A beta band is a frequency band of 14- < 30 Hz with waves of 33–72 ms duration and amplitude mostly below 30 μV and is the base of beta rhythm, which is defined as any EEG rhythm within that range of frequencies. Typically recorded over fronto-central regions of the scalp during wakefulness and may be induced by some drugs like alcohol, barbiturates, propofol, and benzodiazepines [32, 33, 35, 36, 47].

1.1.4 Gamma (γ) activity

The gamma band includes frequencies from 30 to < 80 Hz, with waves with a duration between 12.5 and 33 ms. Gamma rhythms are ubiquitous in many brain regions, particularly in the hippocampus and neocortex, and are related to many cognitive processes [36, 48].

1.1.5 Theta (θ) activity

Theta waves are defined as occurring within the frequency range of 4 to < 8 Hz with a duration of 125–250 ms, with origin in hippocampal, hypothalamic and limbic interneuronal networks. Theta oscillations have a double, paradoxical connection with drowsiness and with intense cognition, and occurr in the frontal midline region during intense

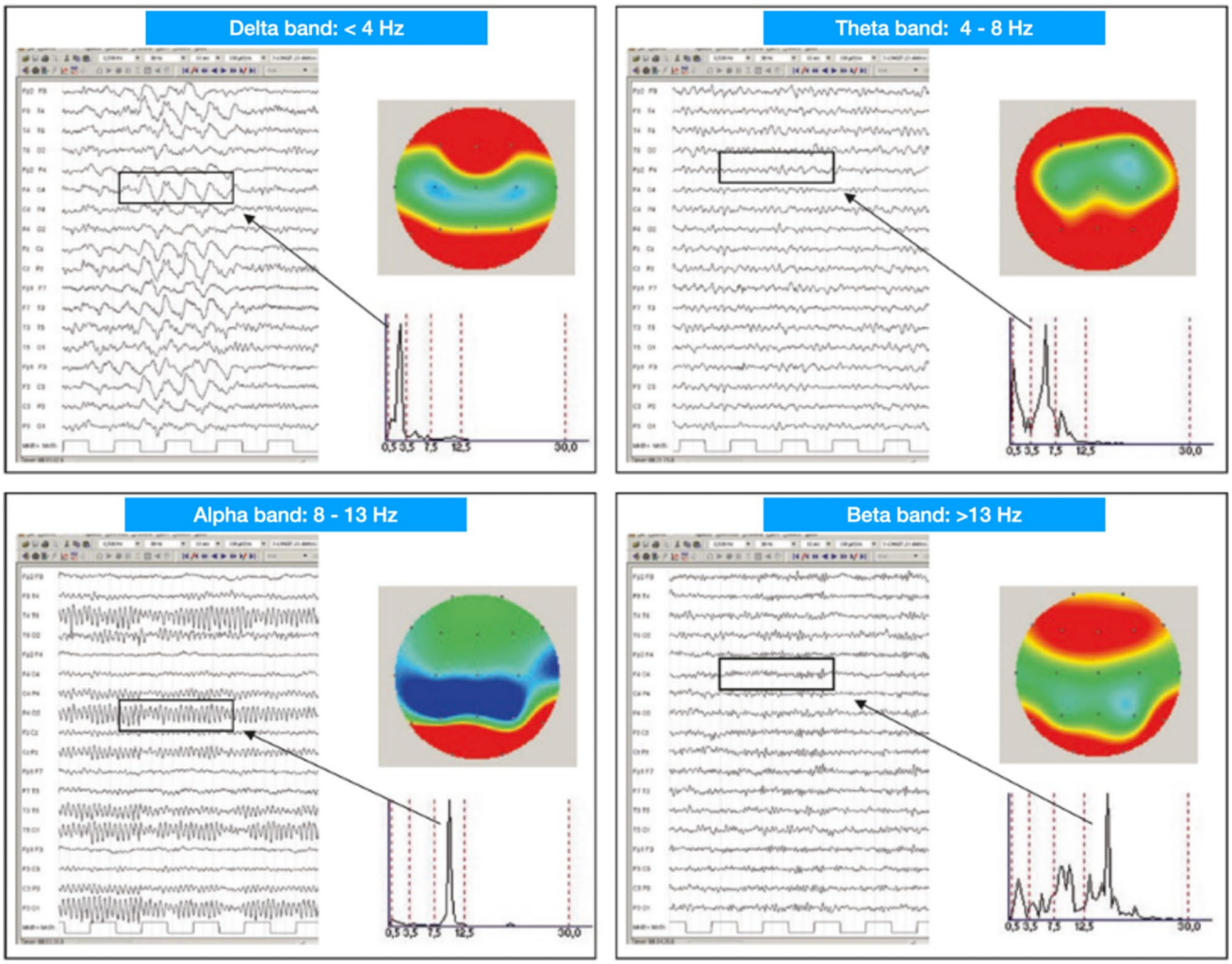

Fig. 2 Qualitative, dominant topographical distribution and spectral representation of the main electroencephalographic frequency bands. Adapted with permission [34].

cognitive tasks [49, 50]. Hippocampal theta waves may also participate in the hypothalamic modulating pathways of the heart rate [51, 52].

1.1.6 slow-delta (δ) activitySlow - delta () activity

The delta waves are oscillations with thalamic and cortical origin, with a duration of 250–2000 ms, and have the lowest frequency (0–4 Hz) and highest amplitude of the classical brainwaves. They appear in stage 3 sleep state and are the dominant oscillations in stage 4. In the awake state, they are considered normal in young children and older adults [36] and have an important role in the integration of cerebral activity with homeostatic processes [53].

1.1.7 Burst suppression

Burst suppression (BS) is an electroencephalographic pattern with high-voltage bursts alternating quasi-periodically with periods of voltage-suppressed activity (Fig. 1 and 4). Recently, the American Clinical Neurophysiology Society (ACNS) defined BS in adults as a EEG background with more than 50% of attenuation (≥ 10 μV but $< 50\%$ of the background voltage) or suppression (< 10 μV9; bursts should have at least 4 phases and last for a minimum of 0.5 s (up to 30 s) [54]. Burst suppression is a nonspecific pattern indicating diffuse cerebral dysfunction. It is usually observed in severely pathological states, including neonates and infants with severe epileptic encephalopathies, hypoxic-ischemic injury, metabolic or infectious encephalopathies, or hypothermia. Still, it can also be observed under the effect of high doses of general anesthetic drugs, representing a low-order dynamic mechanism [55].

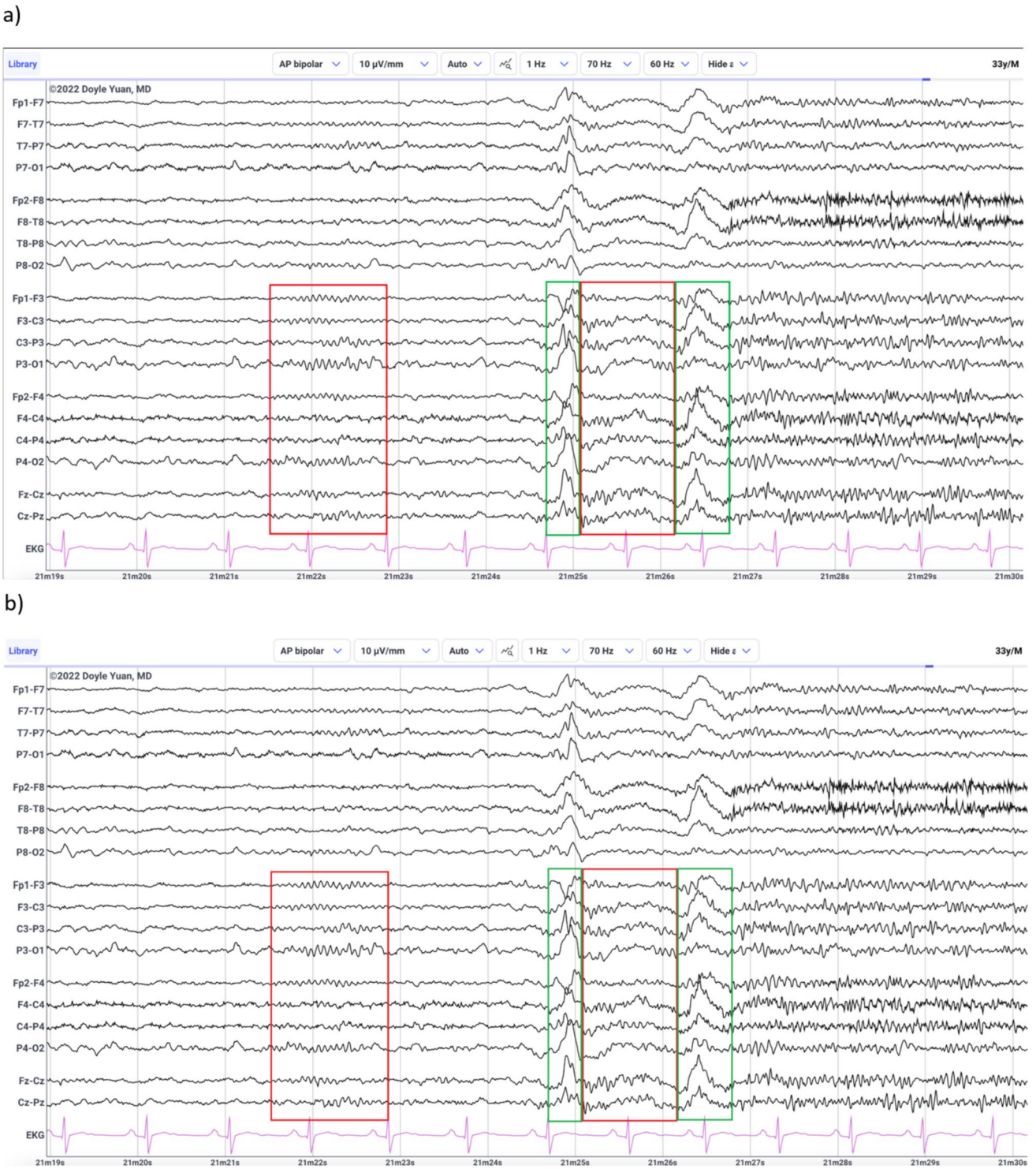

Fig. 3 Spindles (red boxes) are comprised of an 11–16 Hz low amplitude oscillation predominating in a frontocentral distribution. They may occur spontaneously or in quick succession with a broad, diphasic, centrally maximal delta waveform called a K-complex (green boxes). These two waveforms are the electrographic hallmarks of non-REM stage II sleep but may also be observed in deeper stages of sleep. They are readily visualized in both average referential (**a**) and longitudinal bipolar (**b**) montage

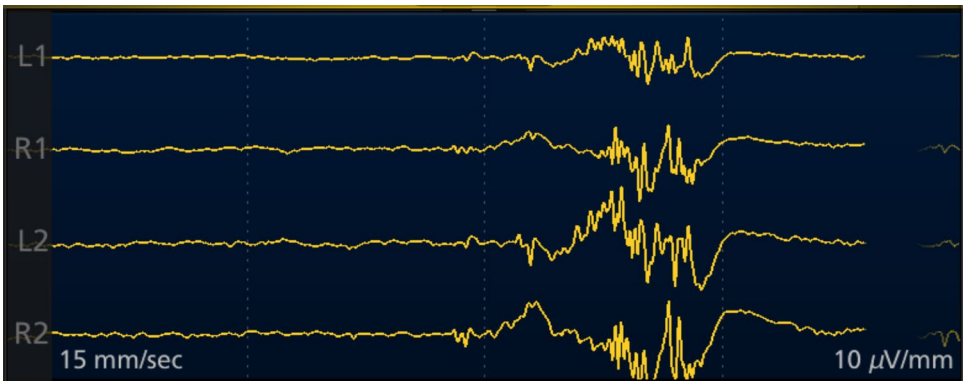

Fig. 4 Burst suppression pattern

A recent systematic review of human and animal literature showed that BS induced by anesthetic drugs was associated with a decrease in cerebral blood flow (CBF) and cerebral metabolism (CMRO2) with a variable effect on cerebral autoregulation [56]. The regional differences of CBF, cerebral metabolism, and the coupling between both [57, 58], in conjunction with the heterogeneity of BS cerebral topography [59], facilitate potential regional harmful mismatch and uncoupling between demand and supply with pharmacological induction of BS as a neuroprotective strategy for anticipated ischemic insult [55] or eventually in cases of status epilepticus [60].

1.2 Electrodes placement systems, channels, and montages

EEG activity varies significantly depending on the area of the scalp from which it is generated. Therefore, regional cerebral rhythms should be recorded using multiple electrodes and recording channels in a standardized system. The International 10–20 system [61, 62], universally used, is achieved by tracing imaginary lines, starting from specified anatomical landmarks and creating circumferential lines mutually perpendicular, one anteroposterior sagittal midline connecting the nasion to the inion through the vertex and a latero-lateral coronal line from the right to the left pre-auricular points through the vertex too (Fig. 5). Along the antero-posterior line, five positions are defined:

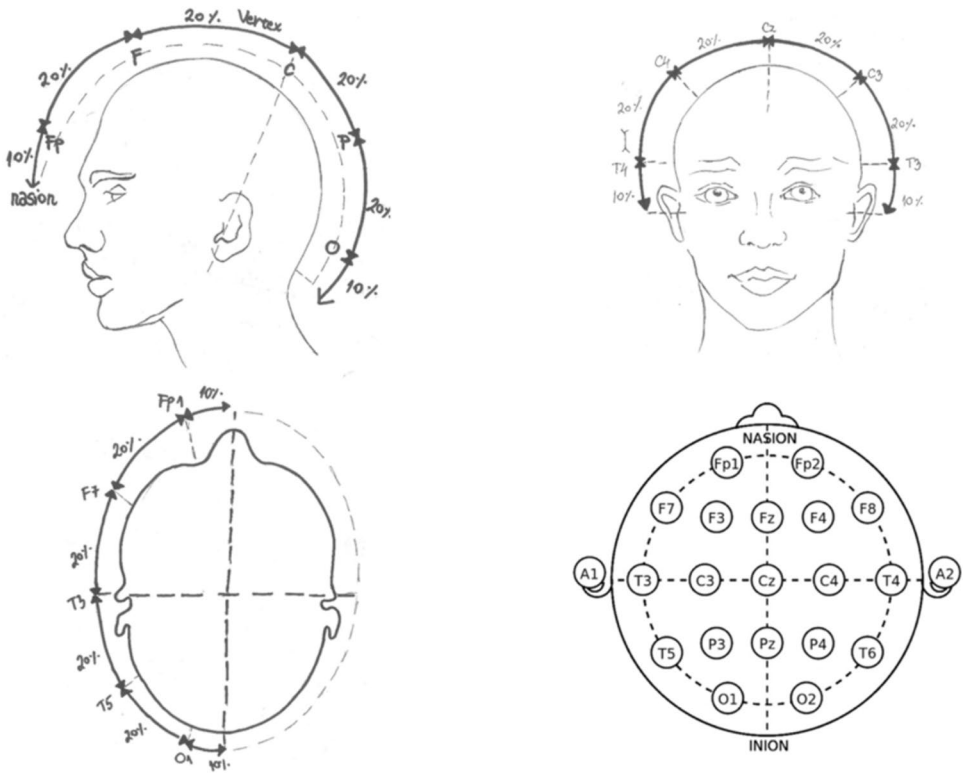

Fig. 5 Electrode locations of International 10–20 system for EEG recording (**A**) Lateral view of skull showing the measurements from the nasion to the inion at the midline. Fp is the frontal pole position, F is the frontal line of electrodes, **C** is the central line of electrodes, P is the parietal line of electrodes, and O is the occipital line. **B** Frontal view of the skull showing the measurement for the central line of electrodes. **C** Frontal view of the skull showing the measurement for the central line of electrodes. **D** Single plane projection of the head, showing all standard positions. The outer circle was drawn at the level of the nasion and inion. The inner circle represents the temporal line of electrodes. This diagram provides a useful stamp for indicating electrode placements in routine recording

frontopolar (Fpz), frontal (Fz), central (Cz), parietal (Pz), and occipital (Oz); considering the total distance between nasion and inion, Fpz and Oz points are located at 10% of the total length of the line while the other positions are calculated at 20% of the distance between the two points. Equally, along the coronal line, temporal electrodes are placed at 10% of the total distance starting from the preauricular points, while lateral central electrodes are placed at 20% from the temporal points and from the vertex. From these two lines, two other circumferential lines may be traced: a lateral longitudinal line and a parasagittal line. Standard numbering of this 10–20 system has a standardized numbering with even-numbered electrodes on the right side of the skull and odd-numbered electrodes on the left side, identified with letters which are placed: Fp2, F4, F8, C4, T4, T6, and O2 for the right hemisphere and Fp1, F3, F7, VC3, P3, T3, T5 and O1 for the left hemisphere, with the electrode numbers increasing as moving away from the midline (Fig. 5). The Z sites refer to electrodes placed on the midline sagittal plane of the skull (FpZ, Fz, Cz, Oz) and are often utilized as grounds or references (Fig. 5). High-resolution systems use extra electrodes, which are added using the 10% division, located in intermediate sites halfway between those of the existing 10–20 system.

A channel is defined by a complete system for the detection, amplification, and display of potential differences between a pair of electrodes or a computed reference. A montage is one particular arrangement or array of channels on the EEG display, defined by the exploring and reference electrodes; a bipolar montage refers to multiple bipolar channels, with no electrode being common to all channels, while a referential montage consists of referential derivation, i.e., recording from a pair of electrodes with the exploring electrode connected to the input terminal 1 and the reference electrode connected to the input terminal 2 of an EEG amplifier [63].

A recent study using a machine learning-based approach based on electroencephalographic data (relative power of delta, theta, alpha, and beta bandwidths) from 30 patients undergoing minor elective surgery under general anesthesia with a 32-channel EEG system, showed that F8 is the best channel to discriminate the states between awake and anesthetic unconsciousness whereas central, parietal and posterior channels poorly detect the transitions between both states [64].

EEG monitors used during anesthesia process the EEG signal using electrodes placed in the frontal region, which may be inadequate when interfering with the location of the surgical procedure (brain surgery, for example). Several alternative locations for sensor placement have been described, but the only one with a valid neurophysiological foundation is based on infraorbital montages [65].

1.3 Processed and quantitative electroencephalography

The EEG signal is never composed of perfectly regular waves, with changes that reflect the complexities inherent to dynamic brain networks. Nevertheless, the EEG can be characterized by several important features, including its organization, continuity, variability, reactivity, and the predominant constituent frequencies at a given level of arousal. This pattern is classically characterized as the EEG background and may be superimposed by transient disturbances that comprise the EEG foreground. This combination of patterns is well represented in the different electroencephalographic signatures of the anesthetic drugs described below.

The EEG waveforms can be analyzed qualitatively and quantitatively. Qualitative interpretation is operator-dependent and focuses on finding patterns that have clinical correlates. In contrast, quantitative EEG (qEEG) analysis involves applying mathematical techniques to the raw EEG signal with the intent of transforming the data based on specific signal parameters of interest. These methods include rhythmicity, amplitude, frequency, and symmetry-focused analyses, each of which may be leveraged for diagnostic purposes or for guiding therapy, depending upon the clinical context.

As mentioned before, clinically useful frequency bands of the EEG are classified as δ (0.5–4 Hz), θ (4–8 Hz), α (8–12 Hz), and β / γ (12–30 Hz). Generally, as the frequency of the waves increases, the amplitude of the wave decreases. This phenomenon can be explained by the theory of synchronization/desynchronization of neuronal populations [66] based on groups of neurons discharging simultaneously at a fixed rate. These synchronous rhythms result from feedback loops in neuronal circuitry connecting the brainstem, thalamus, and cerebral cortex. However, during cortical activation, these rhythmic discharges are disrupted by individual and asynchronous firing of neurons within these circuits, eventually creating a low amplitude signal (additive effect obviated due to temporal dispersion of the discharges) with a rapid rate (short interval between discharges of individual neurons). Therefore, a gradual change from synchronization to desynchronization is heralded on the EEG by a gradual transition from large amplitude slow activity (δ, θ) to small amplitude fast activity (α, β) and vice versa [10].

1.4 Quantitative EEG

Essentially, the EEG is a voltage–time graph and whatever parameters can be derived directly from that graph are called "time-domain" parameters. When analyzing the time domain, the EEG is segmented into fixed time intervals called "epochs". The length of the epoch can be modified based on the required time resolution of the parameter and how long a segment is required to acquire

the parameter. Epochs are created using "windowing" techniques by which the application of a specific function digitally creates a "window" of the signal within which the values are like the original signal and beyond which the values quickly trail off towards zero [10].

1.4.1 Time domain

Several statistical parameters have been described to analyze the EEG signal as a function of time, including zero-order frequency, aperiodic analysis, symbolic analysis, mean, median, variance, standard deviation, skewness, and kurtosis. With the period amplitude analysis, one can extract the number of waves, wave duration, peak amplitude, and instantaneous frequency [67, 68]. Of all described time domain parameters, possibly the only one with clinical interest in the anesthesia practice is the quantification of the presence of the BS pattern with the burst suppression ratio (BSR), calculated by dividing the EEG into epochs of bursts and suppressions by a voltage-based scale; it progresses from 0 to 1, with 0 indicating no suppression and 1 complete cessation of electrical activity with suppressed EEG [55].

1.4.2 Frequency domain

The frequency domain approach analyses the EEG signal as a function of frequency, mainly using the Fourier transform and the bispectral analysis. Quantitative interpretation of the EEG signal relies on the decomposition in sine and cosine waves, separating the inherent frequencies of the EEG wave. To this end, the most common mathematical tool used is the "Fast Fourier Transform", a transformation of a mixed frequency wave providing three different sets of information: frequencies, amplitude content of those frequencies (known as "power" in spectral analysis), and the phase of those frequencies (Fig. 6). [69]

1.4.3 Band power and band ratio

Since we have information regarding power (amplitude information) of each frequency, the frequencies can be grouped together into relevant bands (β, α, θ, δ), and the relative powers can be summed to provide band power (measured in dB or μV^2). By itself, band power isn't particularly a useful measurement, but if the band powers are divided by the total power of EEG, the "relative band ratio" can be obtained by providing the power distribution of the EEG:

$$\text{Band Ratio} = \text{Band Power}/\text{Total Power} * 100$$

1.4.4 Power spectrum

The graphical representation of power on the Y-axis and frequency on the X-axis is called the power spectrum (PS). The PS helps in observing the power distribution across the frequencies quickly (Fig. 7).

1.4.5 Compressed spectral array and density spectral array

The PS of one channel plotted over time provides a 3-dimensional view of the power distribution of frequencies over time (Z-axis). This is known as a Compressed Spectral Array (CSA) and allows us to observe rapid changes in the power distributions. If the 3-dimensional CSA is turned towards the observer in such a way that the "Time" is on the Y-axis and "Frequency" is on the X-axis, and the peaks of power are also directed towards the observer, then they will appear as dots – higher the peak, denser the dot and vice-versa. This 2-dimensional representation of the CSA is known as Density Spectral Array (DSA).

1.4.6 Color spectrogram

The color spectrogram (Fig. 8) uses a different approach to represent the dynamic change over time of relative

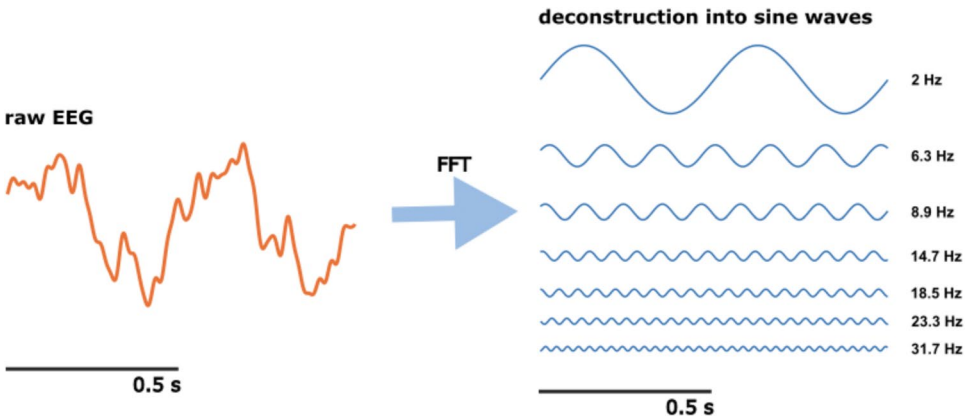

Fig. 6 Representative image of Fourier transform. Using this approach, a variety of indicative frequencies, as well as graphical representations of the power spectrum, can be obtained. (FFT—Fast Fourier Transformation)

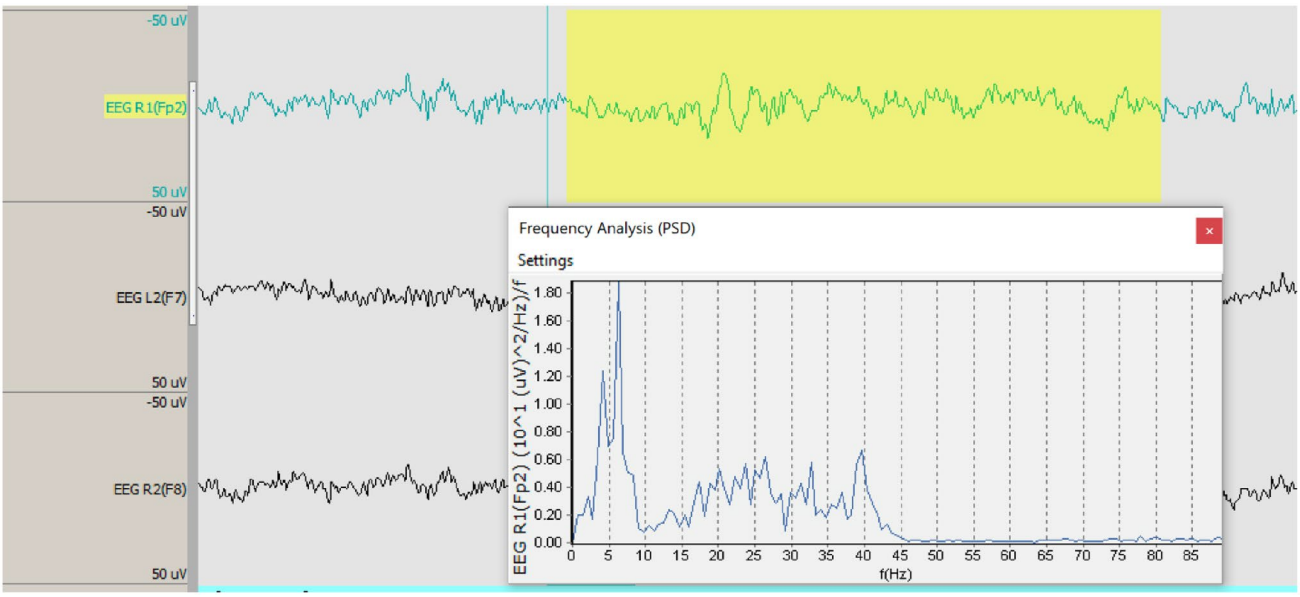

Fig. 7 Power spectral density graph of a short epoch (yellow box) of raw electroencephalogram signal showing higher powers in delta and theta bands, and lower power in the alpha, beta gamma, and higher frequencies. Electroencephalogram: EEG

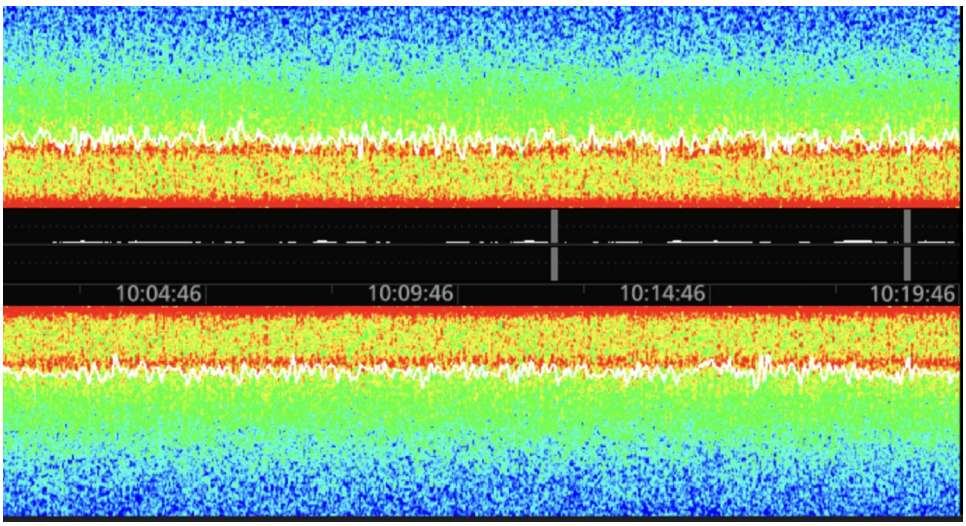

Fig. 8 Spectrogram with propofol anesthesia with dominant power in alpha and delta bandwidths

frequency powers [68]. For a given epoch of raw EEG, the segment is disassembled into its frequency components and again plotting frequency and power, but now using a color scale from red to dark blue, related with more or less power, respectively. Visualization of changes in frequencies, power, and detection of small changes in the frequency structure is easier in a continuous colored spectral analysis. The signature patterns in the spectrogram generated by different anesthetic drugs are reviewed in another section of this article.

1.4.7 Spectral edge frequency

The Spectral Edge Frequency (SEF) is a commonly used qEEG parameter SEF may be defined as the frequency in a power spectrum below which *x* % of total power of the EEG is located, where *x* is usually 75 or 95%. (Fig. 9). SEF may be useful as it can encapsulate changes in power–frequency distribution into a single number: as the power of higher frequencies reduces, the SEF shifts to the right and vice versa. Whereas an awake patient will have SEF in the range of 22- 25 Hz, a moderately sedated patient will have

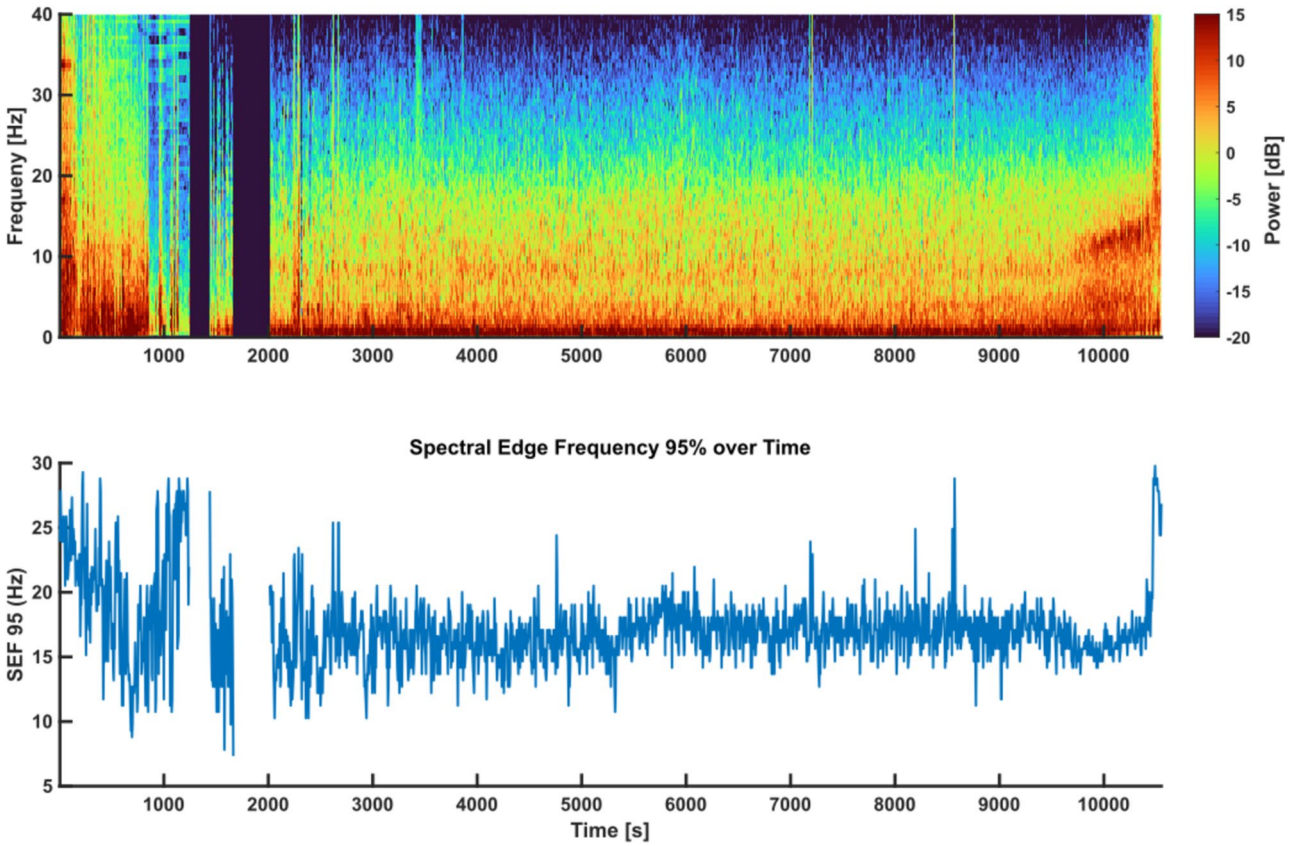

Fig. 9 Trend of Spectral Edge Frequency (SEF) 95% showing initial and final high frequencies corresponding to the awake state and values between 10 and 20 HZ corresponding to the anesthetic state

SEF in the range of 14–18 Hz, with a progressive decrease in SEF in the anesthetized patient to 10–14 Hz, and under deep anesthesia, < 8 Hz. However, the SEF is not a reliable metric to assess the adequacy of anesthesia level if used as a single quantitative parameter [70].

1.4.8 Median frequency

Median Frequency (MF) is the frequency below which 50% of the power of EEG is located. It may be another quantitative parameter used to analyze the power spectrum and can easily be calculated. Usually, the MF of awake subjects is at a level of 12 Hz and, during anesthesia, shifts to lower levels and frequencies of about 2–3 Hz [66, 67]. MF is not a very useful parameter because the magnitude of change in MF due to changes in the power spectrum is minimal compared to SEF.

1.5 Processed EEG-derived monitors

Several monitors have been developed using different approaches to process the raw EEG typically acquired from the frontal region and calculate a dimensionless index, which is related to the level of activation/depression of EEG activity. All these pEEG-derived monitors and respective indices of arousal/unconsciousness resulting from proprietary algorithms share the submarine principle [70], a simplified view of an anesthetic trajectory moving from the top of a full arousal state, which generates an index of 100, to the bottom at a deep state of unconsciousness and electrical cerebral inactivity with an index of 0, throughout travel by a gradual slowing of EEG activity. These monitors and respective scales had the merit to be the first window opened into the brain during anesthesia by clinical anesthesiologists [12]; however, the proprietary, dimensionless numerical scales lack a strong and clear neurobiological background [19] and, in many situations, the calculated index is not correlated with the real level of alertness or with the concentrations of anesthetic drugs. [71–74]

All these monitors have been extensively reviewed [17, 18, 23, 74, 75] and a comprehensive comparison between monitors can be found elsewhere [76]. Briefly, we describe commonly used monitors: the BIS, the M-Entropy® (GE Healthcare, Helsinki, Finland), Sedline® (Masimo, Irvine, CA, USA), Narcotrend® (Narcotrend Group, Hannover, Germany), Conox® (Quantium Medical, Barcelona, Spain/

Fresenius Kabi, Germany)) and NeuroSENSE® (NeuroWave Systems Inc, Beachwood, OH, USA).

1.5.1 BIS – bispectral index

All the techniques described above ignore an essential concept of phase information in the EEG and the phase relationships between various EEG frequencies. These phase relationships may be quantified as the EEG bispectrum, which is normalized as a percentage of the maximal achievable phase coupling (measured as the real triple product) to produce a percentage variable that accounts for changes in amplitude and is termed the bicoherence index. The BIS is a multivariate measure containing features that include the EEG bicoherence, bispectrum, and real triple product, along with time domain features such as the burst suppression ratio. The BIS is a statistically based, empirically derived complex parameter, a weighted sum of several electroencephalographic sub-parameters, including time domain, frequency domain, and high-order spectral sub-parameters [10]. The BIS monitor was the first monitor providing a dimensionless number correlated with the level of alertness, which ranges from 0 (equivalent to EEG silence) to 100, where a BIS value between 40 and 60 indicates an appropriate level for general anesthesia as recommended by the manufacturer.

As with other types of EEG analysis, the calculation algorithm used by the BIS monitor is proprietary, although it has been recently successfully reversed-engineered [72]. Other parameters provided are the Signal Quality Index (SQI), the SEF95, the BSR, a low-resolution color spectrogram, and the electromyography (EMG) activity. In addition to the original two-channels sensor, there is a bilateral 4-channels sensor displaying a graphical index of asymmetry between both sides.

1.5.2 Entropy module

It was proposed that non-linear electroencephalographic dynamics can be used to adequately describe the depth of anesthesia. The Entropy Module is a mathematical concept quantifying non-linear dynamics resulting from a measure of information called Shannon entropy. When applied to the power spectrum of EEG, spectral entropy is obtained and measures the regularity of the frequency distribution [77].

The Entropy Module calculates s two parameters, the Response Entropy (RE) and the State Entropy (SE). The RE is calculated in the frequency range from 0 to 47 Hz and includes EEG and facial EMG (FEMG) activity; this fast reacting RE index varies between 0 and 100 and is sensitive to the activation of facial muscles. FEMG is primarily active during the awake state but may also activate during surgery. Facial muscles may also indicate an early emergence, which can be seen as a brief rise in RE. The SE E ranges from 0–91 and is calculated in the frequency range from 0 to 32 Hz and mainly includes EEG activity. The SE value is always less than or equal to the RE. The State Entropy is less affected by sudden reactions to the facial muscles because it is mainly based on the EEG signal. The desired range of entropy under general anesthesia would be between 40 and 60 [78–80].

1.5.3 Narcotrend

In 1937, Loomis et al. [81] described systematic electroencephalographic changes occurring during human sleep and defined five stages, A–E, to distinguish different EEG patterns. The Narcotrend monitor uses a modified scale with some sub-stages and is applied to the dynamic electroencephalographic changes recorded during anesthesia (stages A = awake to F = very deep level of anesthesia). Several quantitative features from the time and the frequency domain are extracted and processed to identify a subset of EEG variables and ultimately transformed to another dimensionless numerical index scale ranging between 0 and 100 [82, 83].

1.5.4 Sedline

The Root® platform (Masimo) is a multifunctional monitor that incorporates the multivariable Sedline module. The SedLine system acquires data from a 4-channel EEG sensor array placed on the patient's forehead. The EEG signals are analyzed by a proprietary algorithm producing the Patient State Index (PSI); the BSR and the EMG Index are also displayed on the Root monitor. Connected to a 24-bit sigma delta converter with 23 nanovolt resolution, the raw data are processed by multiple feature extraction modules, an integral part of the proprietary algorithm ensuring optimum performance over a wide dynamic range of EEG from pediatric to geriatric patients. It also displays a bilateral colored spectrogram in addition to the 4 channels of raw EEG waves, with the possibility to scale the spectrogram power, the voltage, and the velocity of the raw EEG traces. The PSI values range from 0 to 100, and adequate surgical anesthesia level is within 25 and 50 [84].

1.5.5 Conox

The qCON index, incorporated in the Conox monitor, is an index derived by advanced digital processing of a single channel of EEG obtained through a proprietary sensor placed on the forehead of the patient. The EEG is recorded in real-time wherein the Fourier transform is calculated and fed into a quadratic regressive model to calculate the qCON. The index was built upon the analysis of a large and diverse dataset comprising a thousand patients by means of an Adaptative Neuro Fuzzy Inference System (ANFIS).

The target range for general anesthesia is between 40 and 60 [85, 86]. The other index calculated by the Conox monitor is the qNOX, an index of the nociception/antinociception balance derived from the same EEG epochs but with a different algorithm, though still based on ANFIS; this index predicts the patient's response to noxious stimulation AND its ideal range during general anesthesia is between 40 and 60 with a low probability to respond to noxious stimulation [87].

1.5.6 NeuroSENSE

The NeuroSense monitor uses a wavelet-based decomposition of the EEG signal yielding a proprietary dimensionless quantitative parameter called Wavelet-based Anesthetic Value (WAV_{CNS}). This monitor processes 2 EEG channels and calculates bilateral indices, SR, the EMG power, DSA, spectral powers, MEF, and SEF. An adequate WAV_{CNS} range for general anesthesia is between 40 and 60, with a low probability of occurrence of burst suppression and consciousness [88–90].

1.6 Part II: electroencephalography and anesthesia

After Hans Berger's discovery of EEG signals in humans [91], Gibbs et al. were the first to identify the electroencephalographic changes induced by anesthetic drugs and suggested that the EEG should be monitored during anesthesia [92]. Unfortunately, several decades passed until anesthesiologists witnessed a new global interest in EEG perioperative monitoring with the launch of the BIS by Aspect Medical Systems in the early nineties [10, 11], correlating the level of arousal with a dimensionless scale varying between 0 and 100. During the last three decades, BIS and the succedaneums' similar indices were the targets of a long journey of clinical research to find a clear place in the armamentarium of perioperative monitoring tools, from monitors to avoid intraoperative awareness to monitors with a broader range of indications. EEG monitoring may have a role in improving short-term outcomes, namely time for eye-opening, response to verbal command, time to extubation, time to orientation, lower requirements of vasopressor drugs [93] and time to discharge from the post-anesthesia care unit [94, 95], and long-term outcomes like perioperative neurocognitive disorders and mortality) [16, 55] and in the intensive care environment (sedation titration, detection of ischemic and other neurological events, sleep quality evaluation). [30, 96, 97]

Perioperative neurocognitive disorders (PNDs) result from the failure of a vulnerable brain to adapt to the acute stressors associated with anesthesia and surgery [98–100]. Several studies have explored the potential of EEG monitoring to identify the brain at risk [98, 101] and to help prevent the development of PNDs [100, 102], though the findings have been inconsistent [76]. Postoperative delirium, a common PND, has been reported to occur in 2–3% of the general surgical population. However, in high-risk patients, the incidence can rise to 50–70%. This condition is strongly associated with significant functional decline, increased mortality, and higher healthcare costs [98, 102, 103]. Excessively deep anesthesia has been proposed as a potential risk factor for postoperative delirium. Numerous studies have investigated whether anesthesia depth guided by EEG monitoring could reduce the incidence of postoperative delirium and long-term cognitive changes. A recent meta-analysis involving 2,138 patients found that the use of BIS significantly reduced the risk of postoperative delirium on the first postoperatively day and decreased the incidence of postoperative cognitive dysfunction 12 weeks after surgery [104]. Similar results were reported by MacKenzie et al. in a meta-analysis of 2,654 patients, which demonstrated that processed EEG-guided anesthesia was associated with a 38% reduction in the odds of developing postoperative delirium [105]. Despite these promising findings, the ENGAGES trial, which compared EEG-guided anesthesia to standard care, found no difference in postoperative delirium incidence between the two groups [106]. However, other studies have highlighted the benefits of EEG monitoring in the prevention of postoperative neurocognitive disorders, particularly when integrated into a multimodal monitoring approach.

Another possible role for the intraoperative use of the EEG is to detect cerebral ischemia. This has been an area of interest during carotid surgery [107]. Carotid clamping during carotid endarterectomy and balloon insufflation during stenting can impair blood flow through an already stenotic carotid artery. Thus, the perfusion of the brain ipsilateral to the side of the procedure relies on the collateral flow. However, the ipsilateral brain undergoes ischemia if this collateral flow is also impaired. Therefore, it is necessary to monitor cerebral perfusion to detect and reverse cerebral ischemia promptly. Changes in EEG patterns like burst suppression or decreasing values could alert clinicians to detect ischemic insults, thus lowering intraoperative stroke risk [108]. However, EEG disproportionately represents cortical activity at the cerebral convexity and does not detect electrical activity in deeper brain structures where ischemia could go undetected [107].

A meta-analysis including eight observational studies and a cohort of 40,317 assessed the potential association between depth of anesthesia as a low BIS values and mortality. The authors found an association between deep anesthesia and 1-year mortality as measured by a low BIS value (< 40–45) [109]. Willingham et al. studied whether intraoperative EEG suppression could independently predict 90-day postoperative mortality [110]. The results do not support the hypothesis that intraoperative EEG suppression, as a measure of excessive anesthetic administration, could be

an independent predictor of 90-day postoperative mortality. However, the authors found an association between BS for more than 5 min and 1-year mortality if BS was coincident with hypotension (mean arterial pressure < 55 mmHg). This potential association between BS and mortality requires further investigations.

In light of the ongoing debate, there is now widespread consensus that the brain should be monitored during anesthesia. The EEG is widely recognized for its ideal characteristics and neurophysiological foundation, making it a suitable tool for routine use in anesthetic practice. Moreover, it is increasingly acknowledged that the field has reached a point where it is time to advance beyond the use of simplistic, dimensionless scales of anesthetic depth. The focus should now shift toward a more structured and evidence-based approach that utilizes the raw EEG signal and its spectral analysis. This approach would leverage the distinctive electroencephalographic signatures associated with anesthetic drugs and intra-operative events, offering a more precise and informed understanding of anesthetic effects on the brain [12, 13, 111].

1.7 Anesthetic drugs and the EEG

The primary neural targets involved in states of sedation and general anesthesia are the preoptic area, the basal forebrain, the lateral hypothalamic area, the ventral tegmental area, the locus coeruleus, and to a lesser extent, the parabrachial nucleus, the dorsal raphe nucleus, the tuberomammillary nucleus, the centromedian thalamus, and the neocortex [1, 112]. Therefore, it is unsurprising that the electroencephalographic changes occurring during induction, maintenance, and emergence from general anesthesia are related to the dynamic disruptive events generated in these areas [113]. The diffuse increase in the power of slow oscillations and marked decrease in fast gamma and beta bands are generally associated equally with anesthetic drugs and physiological NREM sleep; however, the sleep loss of sensory disconnection is accompanied by widespread EEG changes while the anesthetic unconsciousness is associated with more localized changes, particularly in the anterior and posterior cingulate cortex [114].

Generally, the trajectory from the awake state to the state of general anesthesia induced by stepwise increasing doses of GABAergic anesthetic drugs like propofol is accompanied by a chain of electroencephalographic changes, starting by an initial paradoxical activation of fast beta activity while clinically the patient is with transitory behavior disinhibition, possibly due to interneuron anti-synchrony, GABA1 mediated inhibition of inhibitory inputs from the globus pallidus to the thalamus and brief decrease in slow currents of potassium in cortical neurons [115], followed by anteriorization of a marked alpha rhythm from posterior to anterior regions of the scalp, initially still mixed with some Beta waves, and a final coherent alpha rhythm, spindle-like, superimposed on a slow-delta dominant background. Instead, if a large bolus is given to achieve a faster induction of general anesthesia, a dominant slow-delta pattern should be expected, possibly alternating with some level of BS [13].

Recent advances in clinical neuropharmacology of common anesthetic drugs allow us to integrate their mechanisms of action and respective neural circuits with the different electroencephalographic changes and ultimately help to titrate and individualize anesthetic dosing schemes and optimize pharmacodynamic interactions.

1.7.1 Propofol

Briefly, propofol induces inhibition of cortical pyramidal neurons through interaction with the postsynaptic γ-aminobutyric acid A ($GABA_A$) receptors, impairing the cortico-thalamic communication with enhanced hyperpolarization and promoting the brainstem inhibition and communication with cortical and sub-cortical structures [3]. Consequently, the dose-dependent changes induced by propofol in the EEG are closely related to the dynamic disruption of the normal physiological state of these structures.

During sedation, propofol induces slow-beta oscillations and slow-delta activity, with the beta waves appearing at low, excitatory doses and preceding loss of consciousness during a slow, stepwise induction of general anesthesia [115]. Established adequate general anesthesia state by propofol is marked by the presence of slow delta oscillations with a superimposed alpha rhythm characterized by 10 Hz waxing and waning, asymmetrical spindles [13, 39].

Another unique EEG feature of propofol-based general anesthesia is the phase-amplitude modulation patterns: the trough-max pattern appears during the transition into and out of anesthetic unconsciousness while the peak-max pattern is a hallmark of established unconsciousness [116] (Fig. 10). The occurrence of a frontal slow-delta and alpha pattern during states of connected consciousness [117] is one of the limitations of the dimensionless scales of anesthesia depth and color spectrogram (Fig. 11); however, the inspection of the raw EEG trace and recognizing the different phase amplitude modulation patterns help to differentiate states with responsiveness from states with unresponsiveness, where the peak-max pattern represents a low probability of awareness. With increasing concentrations, alpha activity will decrease towards a dominant slow delta pattern followed by BS. The probability of having BS increases with age and co-morbidities [118–121]. At lower concentrations, there is a shift towards higher frequencies and decrease in the alpha power (Fig. 12).

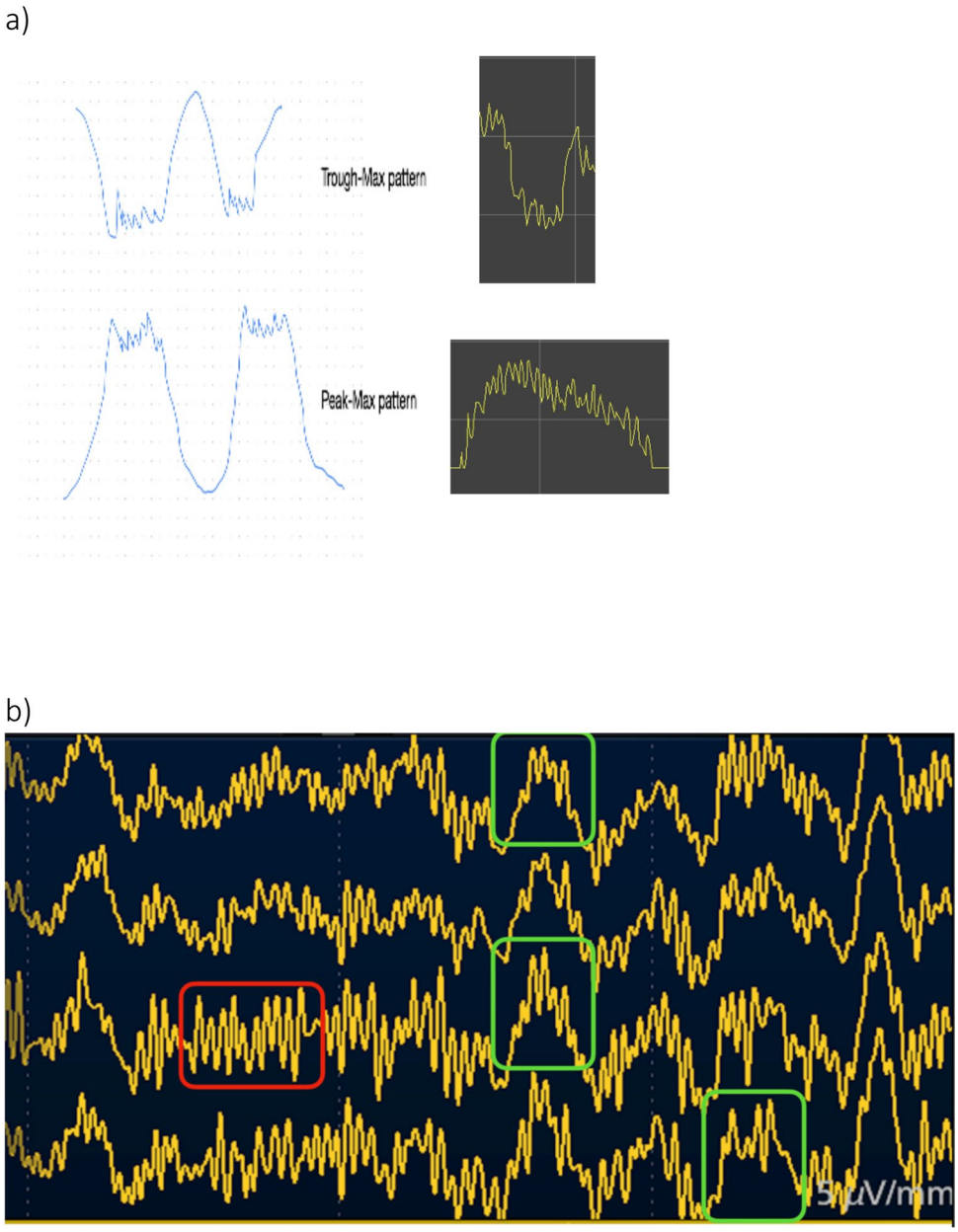

Fig. 10 **a** Trough-max and peak-max patterns; **b** Characteristic raw EEG of propofol based anesthesia with alpha-spindles (red box) and slow delta oscillations with peak-max pattern (green boxes)

1.7.2 Volatile agents

Volatile agents act essentially on $GABA_A$ receptors, glycine receptors, two-pore potassium channels, and N- methyl-D-aspartate (NMDA) receptors [122]. Like propofol, they induce dose-dependent EEG changes, with increased power in slow-delta and beta oscillations at low concentrations, followed, at higher concentrations, by an increase in alpha oscillations (Fig. 13) and an increase in theta oscillations filling the spectra between delta and alpha bands (Fig. 14). A further increase will gradually abolish alpha and theta waves, inducing a slow-delta dominant pattern that may be accompanied and/or replaced by electroencephalographic BS [123–125].

The origin of the characteristic theta waves associated with volatile agents may be related to the effects of inhalational agents on the tandem pore domain K^+ channel TASK-1 channels [126], which are prominently found in the hippocampus [127]. In addition, sevoflurane may increase the rate of spikes, ripples on spikes, and fast ripples on spikes in patients with normal hippocampus and interictal epileptiform discharges from the para-hippocampal [128].

1.7.3 Ketamine

The electroencephalographic signatures of ketamine are related to its ability to bind and block open N-Methyl-D-Aspartate (NMDA) receptors in the brain and are

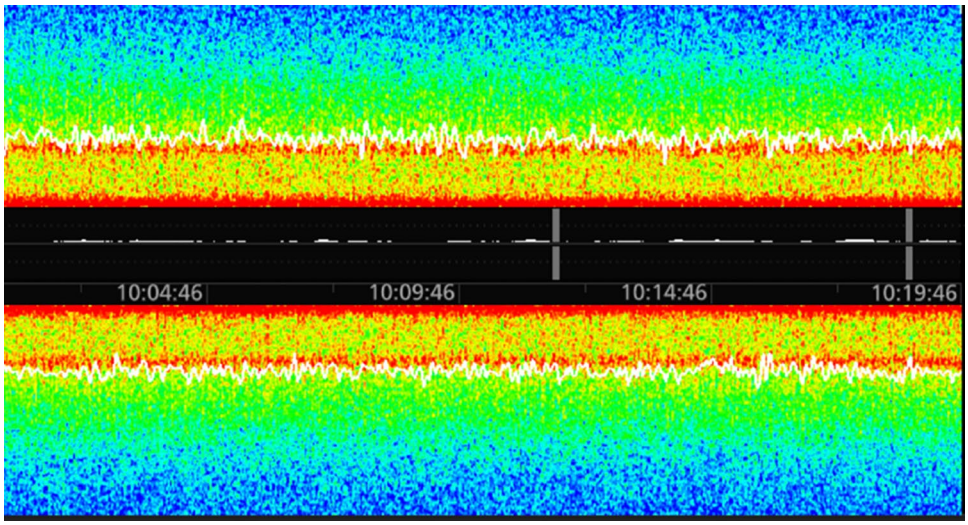

Fig. 11 Typical spectrogram of propofol-based anesthesia with well-defined dominant activity in the delta and alpha bands of frequencies

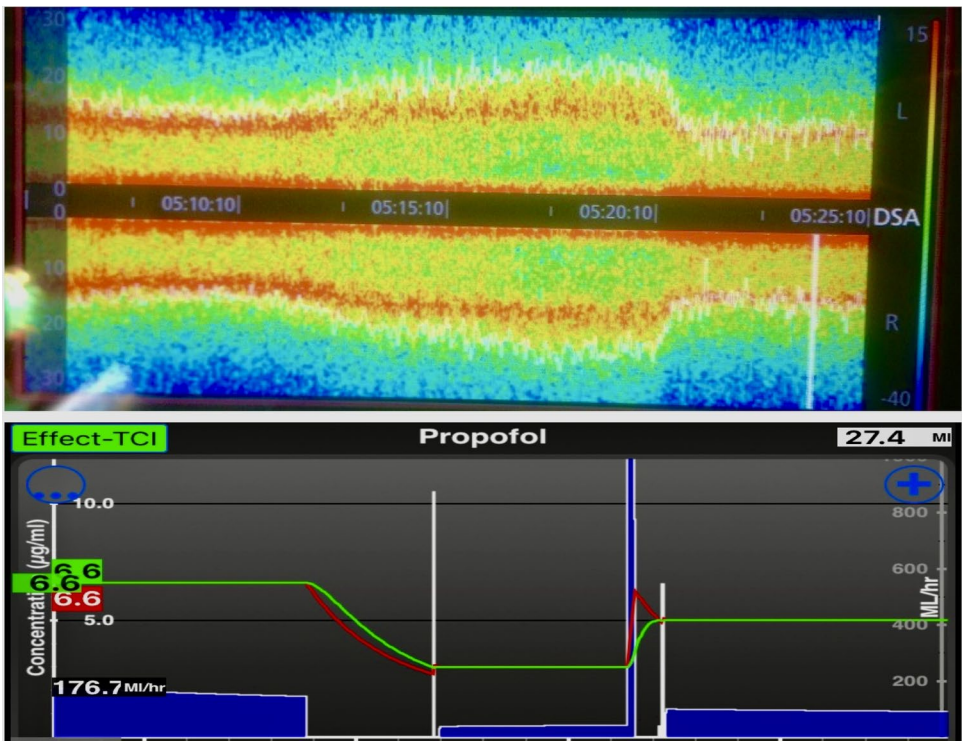

Fig. 12 Spectrogram with three different relative power in the alpha range of frequencies related to different effect-site concentrations of propofol (6.6, 4.5, and 5 µg/mL, modified Marsh Model). Spectrogram by Root monitor. Simulation by Tivatrainer.® software (GuttaBV, Aerdenhout, Netherlands)

dose-dependent. Ketamine increases the EEG power in ranges higher than 20 Hz, with a significant increase of relative beta power with increasing concentrations (Fig. 15). Typically, subanesthetic doses suppress alpha oscillations [129–131], while during the general anesthetic state induced by a bolus of ketamine there is an increase in delta, theta, and gamma power [131, 132] with a characteristic gamma-burst pattern consisting of gamma oscillations alternating with slow oscillations that will be replaced by a stable beta/gamma pattern [133]. Subanesthetic doses of S-ketamine given during sevoflurane-based anesthesia equally decrease the power of slow, delta, and alpha waves and increase alpha peak frequency and the power of beta-gamma bands [134].

Interestingly, the typical changes induced by ketamine disappear or are attenuated when patients have preoperative cognitive impairment [135], suggesting a disruption in the physiological thalamo-cortical circuits. As a result of these effects on the EEG, it is not surprising that ketamine may falsely increase the dimensionless scales of anesthetic level [136–139]; however, Faraoni et al. found that a very low subanesthetic dose of ketamine has no effect on BIS during

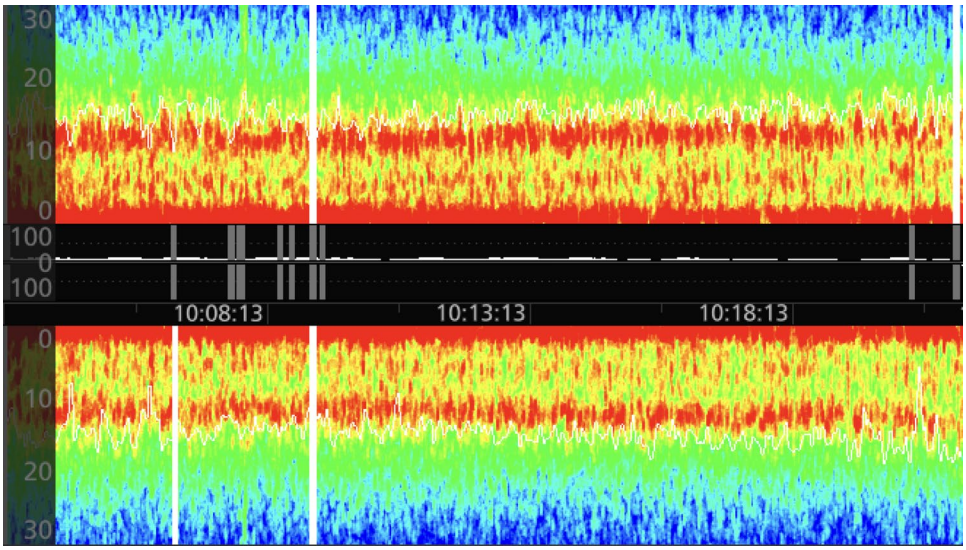

Fig. 13 Spectral image showing the presence of significant power in the theta band with activity also in the slow—delta and alpha ranges. Patient under general anesthesia with sevoflurane at stable 1.4 MAC

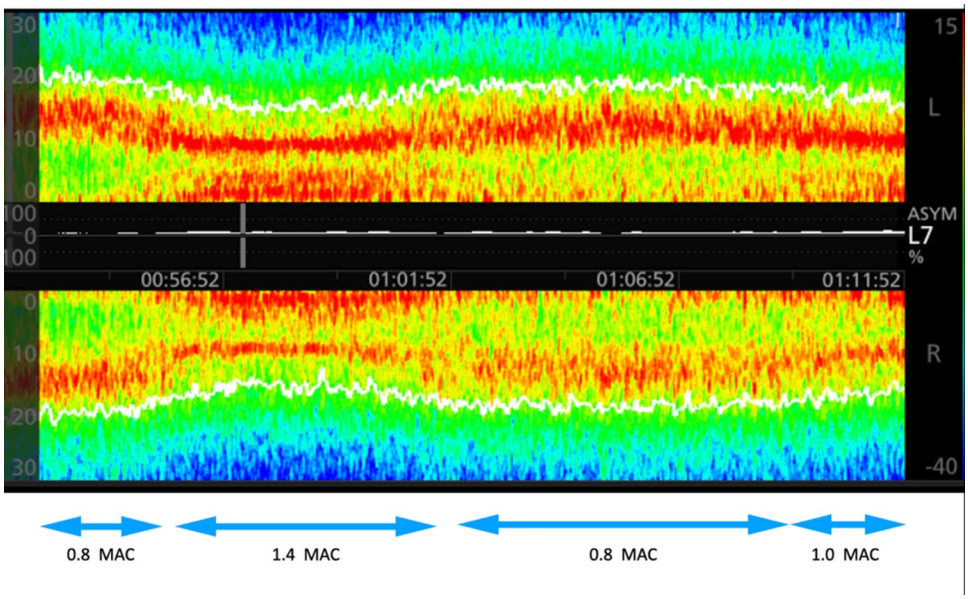

Fig. 14 Dynamic changes in the frontal spectrogram during sevoflurane-based anesthesia at different minimum alveolar concentration (MAC). Initially, a lighter level with 0.8 MAC with bilateral dominant activity between 10 and 15 Hz followed by a marked increase in delta, theta and alpha activity with lack of slow beta activity corresponding to an increase in sevoflurane concentration. At 1 MAC, there is again appearance of activity in the slow delta and theta frequencies with a shift towards a strong alpha activity

stable propofol-remifentanil anesthesia possibly translating the peripheral antinociceptive effect of ketamine [140].

When used concomitantly with propofol or volatile agents, ketamine competes for the same thalamo-cortical inter-neuronal networks and may decrease or abolish the action of the GABAergic drug translated by a decrease in the hyper-synchronic alpha oscillations (Fig. 16).

The use of ketamine is a key component of a multimodal general anesthesia approach [3, 141]. Though being widely used as an antinociceptive drug at low doses [142], ketamine has a significant pharmacokinetic/pharmacodynamic variability [143–145] with a consequent risk of overdose with associated undesirable side effects such as delayed emergence, delirium, and hallucinations. The use of EEG allows the identification of an effective clinical, low antinociceptive dose of ketamine with specific selectivity in the dorsal horn of the spinal cord [146], which shouldn't cause any change in the previously established EEG pattern.

1.7.4 Dexmedetomidine

The electroencephalographic effects of dexmedetomidine are dose-dependent and related to the mechanisms and site of action of this potent selective α_2-adrenoreceptor agonist. Dexmedetomidine binds to presynaptic α_2-receptors in neurons projecting from the locus coeruleus, decreasing the release of norepinephrine, activation of inhibitory inputs to the midbrain, pons and hypothalamus and impairment of excitatory inputs from the locus coeruleus to the thalamus and to the forebrain with a concomitant

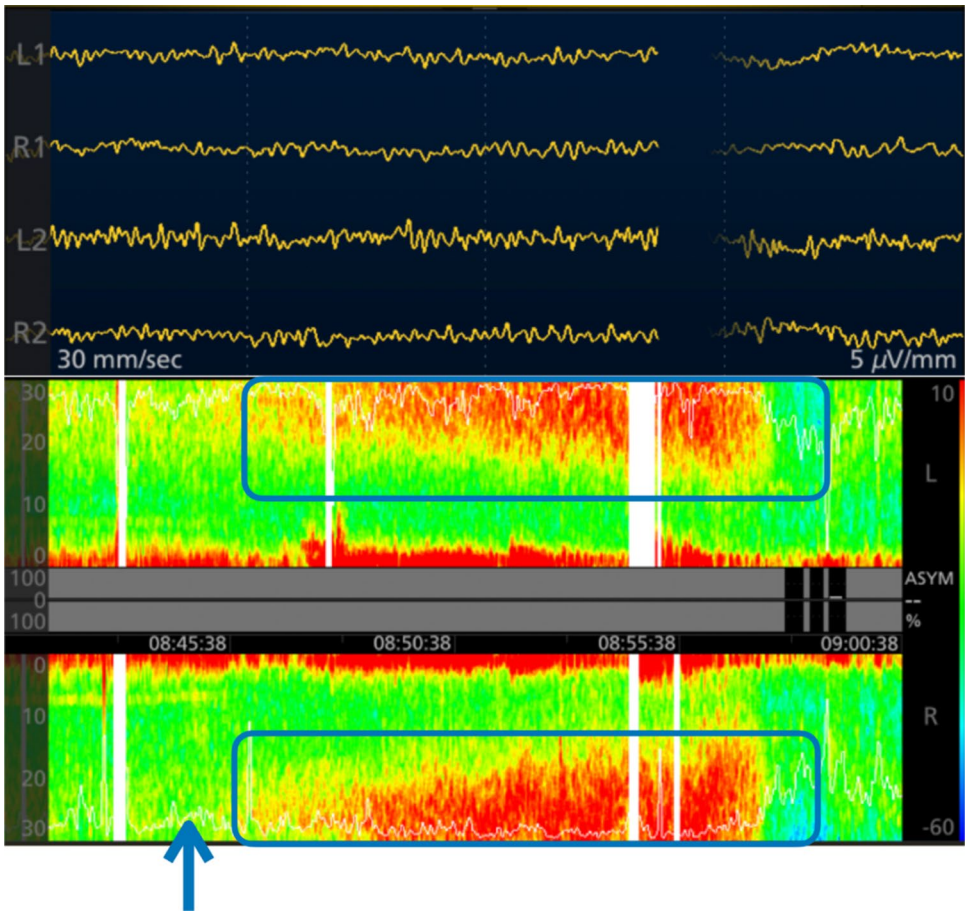

Fig. 15 Effects of a bolus of 1 mg/kg of ketamine (blue arrow) with a transitory increase in the fast beta/gamma frequencies (blue boxes)

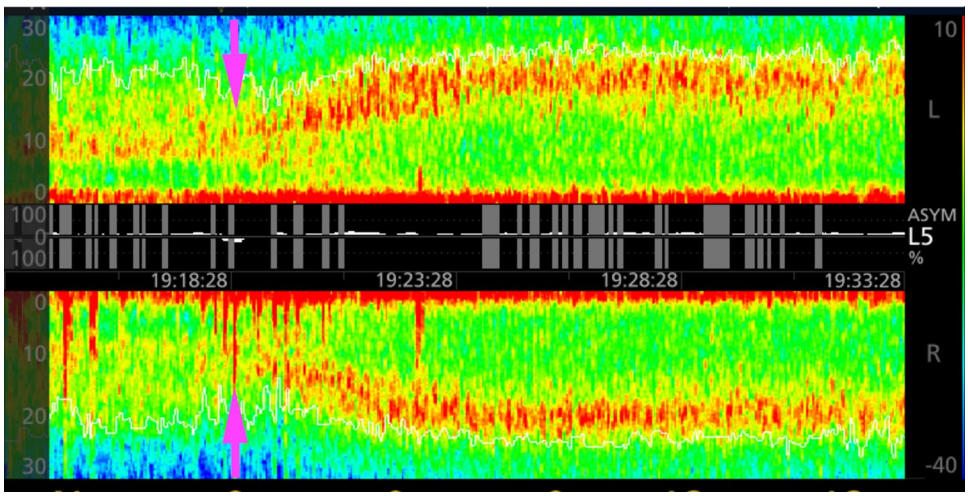

Fig. 16 Spectrogram of a propofol + remifentanil-based anesthesia with a delta-alpha pattern followed by increased activity towards fast frequencies after a bolus of 0.6 mg/kg of ketamine (pink arrow)

decrease of thalamo-cortical connectivity [147]. Beyond these "central" effects,dexmedetomidine acts as an antinociceptive agent in the peripheral nervous system through a dose-dependent suppression of C-fibers and Aα-fibers and inhibition of nociceptive neurotransmission within the posterior horn of the spinal cord [148, 149]; furthermore, dexmedetomidine facilitates the release of acetylcholine from spinal interneurons and increases nitric oxide production. [150].

The sleep-like state induced by dexmedetomidine is characterized by EEG activity similar to the physiological stage N2 sleep with marked spindle activity demonstrating

maximum power and coherence at 13 Hz in the frontal regions, increased theta oscillations in the posterior regions, and increased slow-delta oscillations in the entire scalp [43, 151–153]. Sleep spindles are similar during dexmedetomidine sedation and normal sleep [42, 46], which may help to differentiate the dominant drug's effects when dexmedetomidine is administered with propofol as a component of multimodal general anesthesia [12, 44, 45] (Fig. 17). The spindles generated by propofol have a typical asymmetrical shape with a baseline shift or, alternatively, are superimposed upon a slow wave; they usually have two or three waxing and waning oscillations separated by a "breaking point" with a higher frequency component at twice the dominant frequency of the spindle [41]. The lower power of spindles of dexmedetomidine, resembling those of stage 2 sleep, are represented in the spectrogram by thin vertical, non-continuous lines between 9 and 15 Hz [46] (Fig. 18).

1.7.5 Opioid drugs

The effects of opioid drugs on the EEG were recently reviewed [154, 155]. Generally, increasing doses of opioid drugs used during anesthesia induces an increase of power of slow delta and theta oscillations with a concurrent downward shift in the 95%SEF. [154, 156, 157]

It is relatively uncommon in clinical anesthetic practice to encounter situations with isolated use of opioid drugs with EEG monitoring. In a recent experimental study, however, a marked increase of the power in the theta and slow/delta bands was demonstrated after a stepwise administration of two or three doses of 2μg/Kg of ideal body

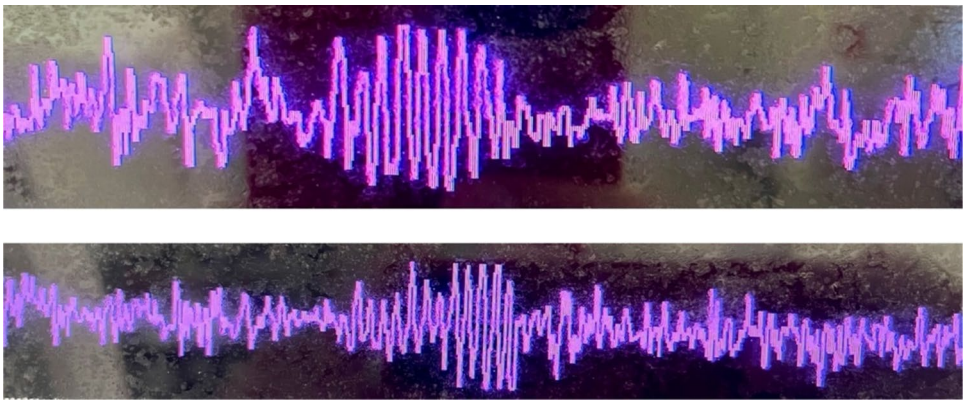

Fig. 17 Differences between spindles induced by dexmedetomidine and propofol. On the top, spindles generated by dexmedetomidine at effect-site concentration of 0.5 ng.ml^{1} (on the top), resembling the sleep spindle, and the more asymmetrical spindle induced by propofol (on the bottom), with a typical "breaking" waxing and waning double oscillation. When combining propofol and dexmedetomidine, we may separate the respective effects by the predominant spindle activity. Reproduced with permission [45].

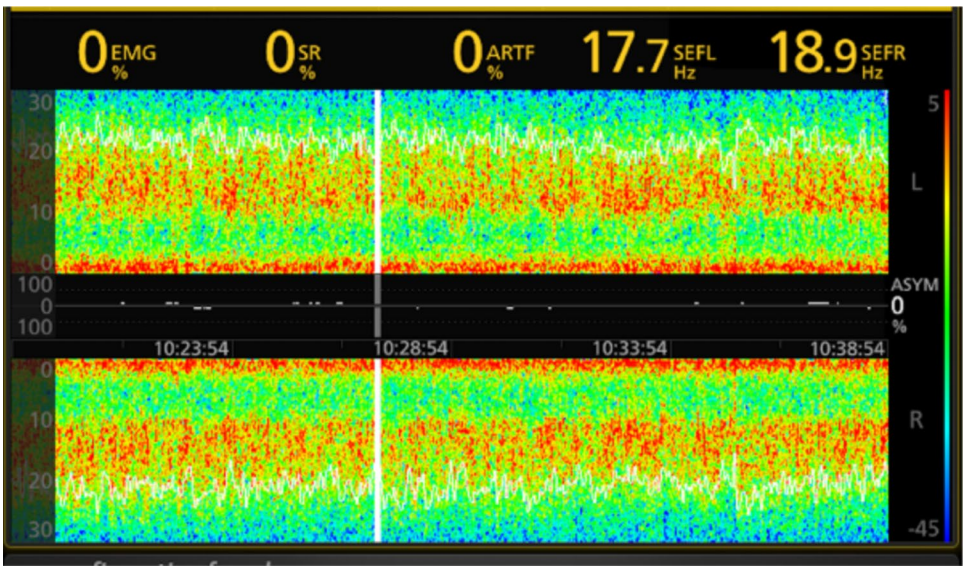

Fig. 18 Bilateral spectrogram derived from a bilateral frontal montage with four electroencephalogram channels showing predominant activity within delta and alpha-slow beta frequencies resulting from a Target Controlled Infusion of dexmedetomidine with a low effect-site concentration of 0.4 ng/mL. Note the values of the SEF95% of 17.7 and 18.9 Hz. EMG: electromyography; SR: suppression ratio; SEF: Spectral Edge Frequency

weight of fentanyl; interestingly, the theta activity was correlated with impaired ventilation and reaction time while the presence of slow/delta oscillations was associated with loss of consciousness [158].

The effect of remifentanil on the electroencephalographic signal has been extensively studied. Using the most common pharmacodynamic model for remifentanil [159], i a sigmoidal decrease in SEF95% was observed with the increase in effect-site concentrations of remifentanil with the inflection point at 4 ng/mL. The increase in slow delta activity induced by remifentanil is predominantly localized in the frontal, fronto-central and fronto-temporal brain regions (areas typically associated with the cortical processing of pain and cognition [160]. Consequently, it has been showed the BIS values decrease with remifentanil independently of nociceptive stimuli like endotracheal intubation and surgical incision [161].

1.8 EEG and nociception-antinociception balance

Pain and the underlying dynamic physiological process of nociception triggered by the noxious stimulus have marked effects on the brain, particularly in the somatosensorial, prefrontal, cingulate cortices, insula, thalamus, and brainstem [162] leading to the identification of numerous pain-related biomarkers in the brain [163]. It is to be expected that surgical nociceptive stimuli and antinociceptive drugs like remifentanil elicit brain activity at various frequencies, thereby facilitating the information exchange among those brain regions [164]. In awake subjects,following painful stimulation, there is an initial shift of fast gamma waves from the brain regions linked to sensory processes to areas that are engaged in emotional experiences [165].

During surgery and anesthesia, a nociceptive stimulation may have a marked effect on the EEG with three possible responses [166–174]:

- a classic beta arousal with an increase in the power of frequencies between 12 and 25 Hz associated with an increased expression of aminergic and cholinergic systems and along with the depolarization of the thalamicortical system; this beta arousal pattern occurs when the level of anesthesia is not so deep with insufficient antinociception;
- alpha dropout represents the loss of the power of a previously established alpha pattern due to thalamic depolarization with partial recovery of thalamo-cortical connectivity (Fig. 19);
- delta arousal is characterized by an increase in the power of slow, delta oscillations in frontal regions concomitantly with loss of alpha activity and is more common during body cavity surgery under volatile-based anesthesia; the mechanisms underlying this delta arousal are not fully understood but possibly involve the modulation of visceral pain pathways on mesencephalic, thalamic and brain stem structures with potentiated negative feedback loops.

Perioperative multimodal monitoring, combining EEG with other nociception monitors [175, 176], allows individualization of different requirements of anesthetic and antinociceptive drugs [177] contributing to better outcomes [178].

1.9 Age and anesthesia: implications for EEG

Normal neonatal EEG changes along the conceptional age and is characterized by the presence of hypersynchronous bursts and occipital slow delta oscillations of 0.5 – 1 Hz between 24 and 27 weeks; occipital delta waves, central delta brushes, rhythmic temporal activity, and sharp temporal theta bursts between 28 and 31 weeks; frequent occipitotemporal delta brushes, synchronous occipital delta waves and rhythmic temporal alpha bursts between 32 and 34 weeks; the presence of the occipital delta brushes started to

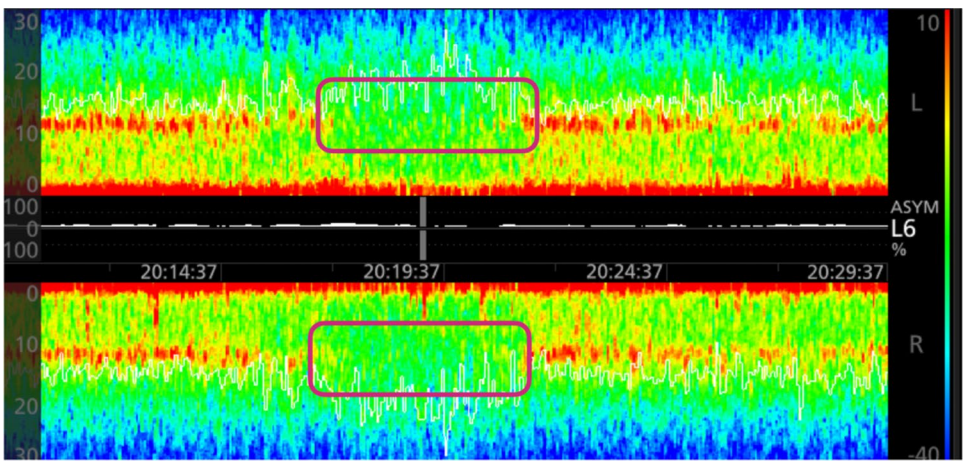

Fig. 19 Transient bilateral alpha drop-out (purple boxes) corresponding to a nociceptive stimulation during propofol + remifentanil-based anesthesia for spine surgery. Effective antinociception was achieved with an increase in the effect-site target concentration of remifentanil

be less frequent between 35 and 27 weeks and are replaced by multifocal slow sharp waves; later, between 38 and 44 weeks of conceptional age, there are rolandic and temporal sharp waves and the EEG is clearly reactive to stimulation with four different behavioral states of wake, active sleep, quiet sleep, and transitional sleep [34].

During the first 3 years of life, the EEG during wakefulness is characterized by diffusely slow, high amplitude delta-theta activity, mainly in central and parietal regions. During the 3rd year of life, an immature alpha rhythm with frequencies between 7 and 8 Hz is seen in the posterior regions during the relaxed, alert state. Between 3 and 5 years old, the posterior rhythm is dominated by frequencies around 8 Hz with marked theta activity in anterior regions at 5–7 Hz. Between 6 and 15 years old, the alpha rhythm reaches 10 Hz but still with medium amplitude and mixed with theta activity. The EEG reaches the fully mature adult pattern at 18–20 years old and persists until the 50th decade, when there is an increase in theta activity and a slight decrease in the alpha power. After 60 years old, there is a significant increase in the theta activity, mainly over the temporal regions, a decrease in alpha activity with progressive global loss of amplitude, a slowing of the background activity and a loss of beta power over precentral regions - particularly within the frequencies between 25 and 30 Hz [34, 179, 180].

As a result of the physiological changes in the brain and respective EEG findings along the life span, from the neurodevelopment process of thalamo-cortical circuits in young ages [181] to the structural, biochemical, and molecular changes that occur with aging [182], the electroencephalographic signatures of the anesthetic drugs also have significant differences. Children up to 3 years old under sevoflurane show slow delta oscillations across all ages, while frontal alpha activity only appears after the 4th month of age and becomes coherent and persisting during anesthesia around 10 months [183–186]. Under propofol-based anesthesia, patients between 0 and 21 years old show age-dependent electroencephalographic features in the delta and alpha oscillations and in coherence [187]: in patients between 1 and 21 years old, there are coherent frontal alpha oscillations which are not present below 1 year old, with an increase in slow coherence with age reaching a peak around 14 years old; frontal slow oscillations have peak power at 11–12 years old and frontal alpha power peaks at 7 years old. In infants less than 1-year-old, the dominant EEG activity induced by propofol falls within the range of slow oscillations; alpha–beta activity can be seen at approximately 5 months of age but only becomes coherent after 1 year old, reflecting the development of thalamo-cortical networks [188, 189].

At the other end of the age spectrum, EEG power across all frequencies bandwidths tends to decrease with both propofol and volatile anesthetics, with specific alterations in alpha oscillations. Of note, there is a greater reduction in alpha activity compared to other frequencies, along with a loss of alpha frontal coherence, and a lower peak coherent frequency [184, 190–192]. Notably, alpha power decreases more than slow oscillations, particularly with propofol [183]. In addition, variation in EEG power spectral density and alpha-delta phase coupling is weaker in older patients under anesthesia with sevoflurane [193]. Elderly patients are also more susceptible to experiencing episodes of burst suppression [119], especially under propofol anesthesia [194]. Furthermore, the amplitude of bursts is also influenced by age, showing a decrease in patients above 65 years when anesthetized with general anesthesia induced with propofol and maintained with sevoflurane.with a decrease observed in subjects over 65 years old under general anesthesia induced by propofol and maintained by sevoflurane [192].

It is not surprising that dimensionless EEG-derived anesthesia indices are affected by age as they compute the signal into a single number using power and relative power in the slow, delta and alpha and beta bands in addition to quantitative measures of burst suppression and the algorithms used do not account for the physiological changes in the EEG with aging (Fig. 20). Globally, the performance of pEEG monitors improves as age increases in children [195–199]; for example, between 6 months and 12 years, BIS increases paradoxically when the end-tidal concentration of sevoflurane increases [200]. With aging, the monitors may miscalculate an elevated index, paradoxically increasing with an increase in the dose of anesthetic drugs [201, 202]. Recently, Obert et al. [72] showed that the PSI calculated by the SedLine monitor increases by 2 index points per decade of age. The changes induced by aging in the amplitude of bursts during burst suppression may further contribute to incorrect calculation of the BSR, a parameter used to quantify the presence of BS based on the detection of periods of suppressed EEG within a pre-defined epoch of time [192].

1.10 EEG and transitional states of consciousness during induction and emergence from general anesthesia

Identification of the moment when loss of consciousness occurs during induction of General Anesthesia and prediction of recovery of consciousness during the process of emergence from general anesthesia are important clinical anesthetic goals [203]. When a patient is put under or emerges from general anesthesia, the EEG changes in distinct ways. Usually, the awake frontal EEG is dominated by relatively high frequencies (beta and gamma bands) and low amplitudes. When a patient closes their eyes and may be able to relax, the amplitudes can increase, and a dominant rhythm in alpha-band frequencies develops. One may consider recording preoperative EEG baselines

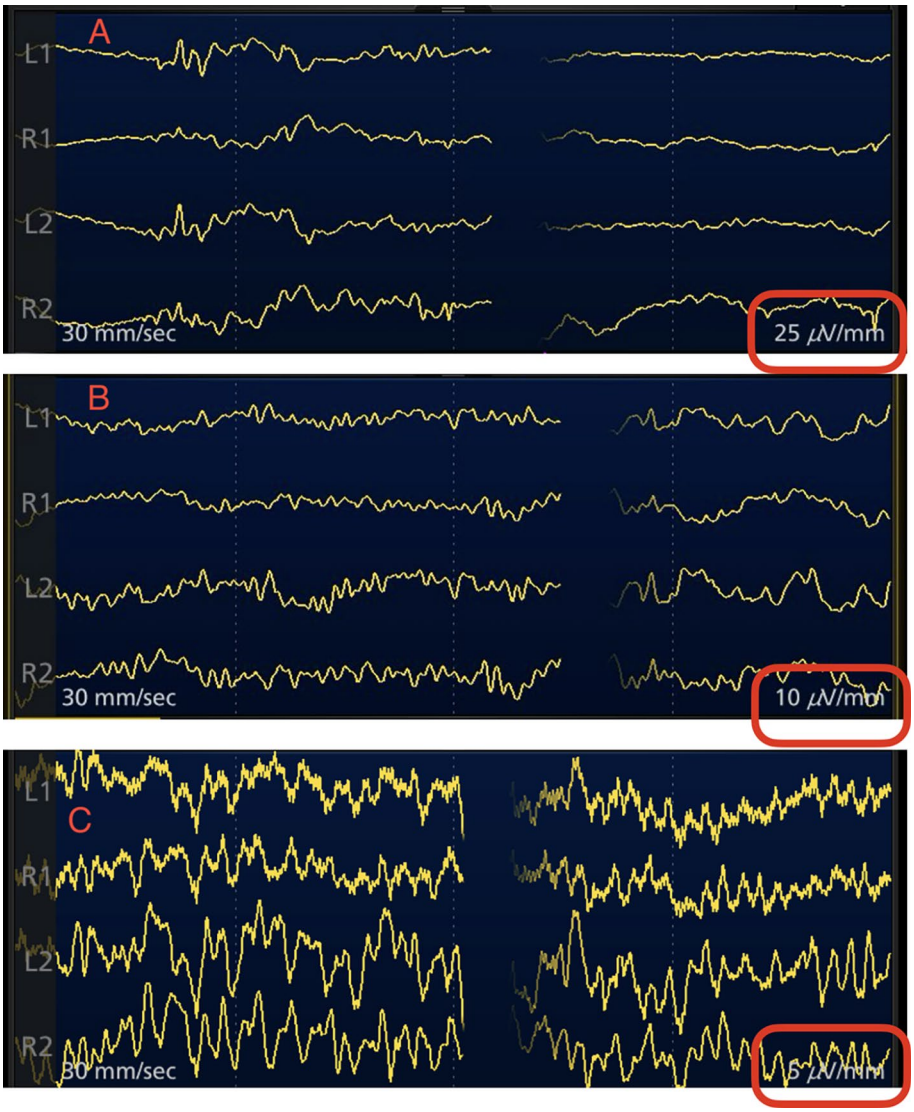

Fig. 20 Raw frontal EEG of a 82 year old patient under propofol anesthesia. A – very low amplitude of the EEG resembling suppressed EEG with a scale of 25µV/mm; B – with adjusted scale to 10 µV/mm it is possible to observe better the real EEG signal, which is very well defined at C with a scale adjustment to 5 µV/mm

as they may already carry information about a potential postoperative cognitive disorder risk [101, 204, 205]. When anesthesia is induced, the EEG pattern typically changes to a slower EEG with dominant activity in the delta and alpha range after the loss of responsiveness. However, before these slow rhythms fully develop, the patient can transverse through an episode with dominant activity in higher frequencies, especially in the beta range (Fig. 21). This has been termed "paradoxical excitation" as the patient may show signs of agitation, and the processed EEG indices may increase [115]. Recent results show that this EEG activation may not be truly paradoxical but may be the first step into EEG synchronization as it can be described by a monotonous decrease in the permutation entropy, a measure of the unpredictability or randomness in the EEG signal [206]. In many cases, a propofol bolus is used for induction, which will lead to unresponsiveness in a matter of seconds. Hence, these changes happen quite abruptly, and a drug overshoot can cause episodes of excessively deep anesthesia characterized by burst suppression. Studies that used slow(er) induction of propofol report a lower incidence of burst suppression, and there is ongoing research about the detailed characteristics of the excitation phase as it can be observed in "slow motion" [207, 208]. Therefore, tracking the EEG before and during induction can help to develop a feeling for anesthesia navigation as first insights into the patient's brain state can be obtained.

The EEG in the final period of anesthesia can contain significant information about the brain state and may help to identify patients with a higher risk of developing postoperative cognitive disorders. If the EEG during emergence smoothly changes from the slow, delta-dominant activity to the fast and flat awake EEG while transitioning through a phase with alpha oscillatory activity the patient follows a desired trajectory associated with a low PND risk.

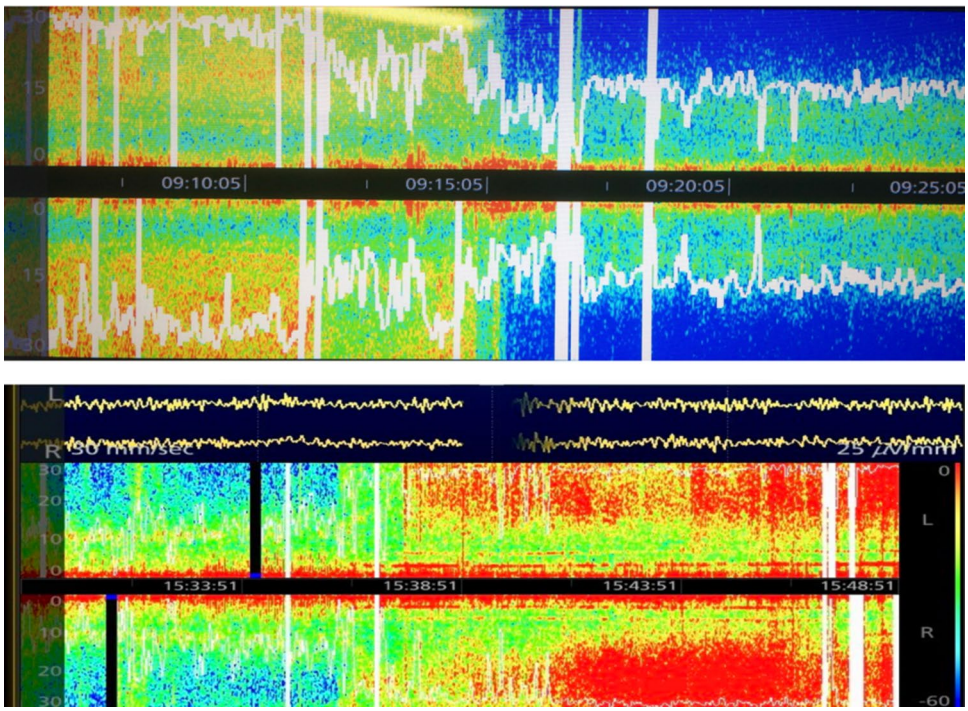

Fig. 21 EEG Spectrogram during loss of consciousness (top) and recovery of consciousness (bottom)

Deviations from this trajectory increase this risk. Especially an emergence EEG that does not change for a long time into emergence and then the patient suddenly wakes up, which is comparable to being ripped out of sleep, the odds for PND increase eight-fold. In general, as during anesthesia maintenance, a strong alpha-band activity during the first part of the emergence seems favorable [209, 210].

1.11 Part III: electroencephalography and intensive care

When a comatose, critically ill patient is admitted to the intensive care unit (ICU), it is current practice to continuously monitor peripheral oxygen saturation, cardiac rhythm, respiratory function, cardiac function, and body temperature, with the goal of having real-time information for every patient [211]. Unfortunately, cerebral function monitoring is often missed even though the brain is a vital organ that is frequently dysfunctional in ICU patients, and its function is usually deeply altered by sedative and antinociceptive drugs. In neurointensive care units (NICU), the patient is usually assessed every 1–2 h for arousal level, motor function, and presence of brainstem reflexes. Still, this approach provides only a snapshot of the patient's neurological status. Furthermore, in non-neurological ICUs, the neurological status is usually assessed once or twice a day. EEG can provide a non-invasive way to assess brain function dynamically. Surface EEG monitoring can be performed over a short duration as a spot EEG (30 – 60 min) [212]. Recent advances in computer technology, networking, and data storage have made continuous EEG (cEEG) monitoring over a prolonged duration, practical, and its use is common in many NICU. The main caveat regarding cEEG is the large amount of data that is time-consuming to interpret and requires specific training. Raw EEG data can be quantified after analysis of fast Fourier transform (FFT) of the signal and represented as total power, ratios of power, or spectrograms obtaining a qEEG trace. These can either be displayed as numbers or graphically as CSA, histograms, or staggered arrays, allowing for rapid screening of long-term recordings [211].

1.12 Application of EEG monitoring in the ICU

There are different medical conditions or situations that may require EEG monitoring for patients in ICU or NICU, and in specific cases, cEEG and/or qEEG:

- Monitoring level of sedation, patient awake but non-responsive or non-awake patients;
- Detecting seizures, non-convulsive Status Epilepticus or subtle motor symptoms;
- Detection and monitoring of metabolic and infectious encephalopathies;
- Monitoring brain function in TBI;
- Detecting intracerebral hemorrhage and occurrence of vasospasm after subarachnoid hemorrhage;
- Monitoring post-cardiac arrest patients;
- Predicting and managing ICU delirium.

1.12.1 Monitoring level of sedation, patient awake but non-responsive or non-awake patients

As described, EEG, especially qEEG, can became a valuable tool in the ICU and NICU in monitoring the level of sedation and for a targeted and controlled patient awakening [213]. In this particular setting, it is possible to use qEEG without cEEG monitoring as long as there are no abnormalities in cerebral activity. For a correct interpretation of raw qEEG data, it is fundamental to strictly correlate the information exported from the BIS monitor (the most studied monitor in ICU settings) or other forms of qEEG with a meticulous clinical evaluation of the patient that takes into consideration the type of anesthetic used, the length of sedation, and baseline neurological background before sedation. When both raw qEEG data and clinical evaluation outline a correct awaken, without any doubt of abnormal electric activity, qEEG monitoring can be dismissed and clinical assessment should guide future medical decisions. On the other hand, if there is any evidence of seizures or if the patient appears to be non-awake or awake but non-responsive, a spot EEG should be performed.Administration of anesthetic agents or antinociceptive drugs should be performed simultaneously with the monitoring of EEG to assess the changes in electrical activity that may explain the underlying clinical state. In addition, EEG monitoring can detect asymmetric electrical activity, including ischemia, intracerebral hemorrhage, and focal seizures. This information can lead to proper diagnostic and therapeutic interventions. It can be of value to use this information with continuous EEG to demonstrate time-related changes in condition. Finally, if the spot EEG shows a symmetrical pattern of diffusely reduced cerebral activity, it would raise the possibility of post-anoxic ischemic injury. In such cases, conventional EEG is usually preferred instead of continuous EEG monitoring.

1.12.2 Detection of seizures, non-convulsive status epilepticus, or subtle motor symptoms

In critically ill patients, there are several etiologies responsible for seizure development, such as acute structural lesions, traumatic brain injury (TBI), infections, intoxications, substance abuse and withdrawal, epilepsy, and metabolic derangements. Clinical indicators can aid the prompt recognition of non-convulsive seizures, such as impaired consciousness, fluctuating mental status, episodic behavioral arrest, focal neurological manifestations, and subtle motor symptoms such as nystagmus, clonus, or opsoclonus [212]. EEG monitoring is widely recommended for the diagnosis of seizures and for monitoring the response to antiepileptic therapy. The most used recording technique is surface recording via 21 electrodes, which uses four bipolar derivations: left and right temporal placements and left and right frontal placements. However, spot EEG identifies only 45–58% of patients who eventually develop seizures [212]. These patients should be ideally recorded for at least 24 h and 48 h if comatose [212].

EEG monitoring during the first 2 h is crucial to identify those patients who may require cEEG monitoring or those in which spot EEG is a more feasible option [212]. The absence of epileptiform abnormalities during the first 2 h of recording is associated with a seizure probability of less than 5% [212]. Of note artifacts can be misinterpreted as seizures in patients admitted to the ICU in a larger percentage of cases compared to patients in the wards. These abnormalities may include physiological alterations, such as eye movements, muscle, sweat, tongue, and pulse movements, but also non-physiological artifacts that are generally 50–60 Hz generated by the surrounding environment (mechanical ventilation and intravenous drips). For these reasons, digital video recording is beneficial in identifying these artifacts.

qEEG enables for the quick review of large amounts of recorded EEG data and unmask subtle changes that occur over many hours. An example of qEEG application for seizure detection in the ICU is a color DSA that displays power measurements for specific frequencies over time. While qEEG is becoming widely available and reliable, invasive EEG monitoring (subdural strips or intracortical electrodes) is not widespread and less used because, despite the higher likelihood of seizure detection, it is affected by remarkable invasiveness and a high rate of side effects.

1.12.3 Detection and monitoring of metabolic AND infectious encephalopathies

Regarding monitoring and infectious encephalopathies, spot EEG is generally preferred over continuous EEG registration. In a retrospective cohort study of patients with primary central nervous system infection who underwent EEG monitoring, electrographic seizures and/or periodic epileptiform discharges were noted in 48% of patients [214]. Periodic epileptiform discharges and viral etiology were independently associated with epileptic seizures. Both electrographic seizures and periodic epileptiform discharges were independently associated with poor outcomes.

1.12.4 Monitoring brain function in traumatic brain injury

In moderate to severe TBI, early and persistently impaired alpha variability on the EEG may be predictive of poor outcomes. Epileptic seizures occur in 20% of patients with severe TBI and are typically non-convulsive [215]. These two findings should trigger the start of cEEG monitoring in TBI patients. Risk factors for seizure occurrence are depressed skull fracture, penetrating injury, and extensive cortical contusions or hematomas. In a seven-day study of

TBI patients, seizures occurred in 22% of patients, and 52% of seizures were non-convulsive despite prophylaxis with antiepileptic drugs s [216]. Another study found a 33% incidence of seizures that occurred approximately 74 h after TBI, with the majority being non-convulsive [217]. On the other hand, EEG reactivity to nociceptive or auditory stimuli predicted better outcomes after TBI, whereas absent EEG reactivity was associated with poor outcomes. This finding had a higher predictive value than the Glasgow Coma Scale or somatosensory evoked potentials [218].

1.12.5 Detection of intracerebral ischemia

Seizures are a well-recognized complication of ischemic strokes. More than 10% of patients with acute ischemic stroke develop acute symptomatic seizures, and up to 30% of these patients are likely to develop epilepsy [218]. Electroencephalography is a sensitive tool for the identification of cerebral ischemia. It can reveal changes in neuronal function, identifying cerebral ischemia in a reversible phase. Continuous EEG monitoring can theoretically identify cerebral ischemia before it is clinically evident, allowing prompt initiation of therapy or imaging studies to prevent irreversible ischemic damage. The detection of delayed cerebral ischemia using cEEG is feasible with high sensitivity in patients with aneurysmal subarachnoid hemorrhage [219].

1.12.6 Post-cardiac arrest and neuroprognostication

cEEG has been recently explored as an alternative technique to clinical examination and to accurately predict clinical outcomes in critically ill neurological patients [220]. Most studies focusing on prognostication were performed in post-hypoxic survivors of cardiorespiratory arrest. A low voltage or isoelectric EEG 24 h after cardiac arrest predicts a poor outcome with 100% specificity (Fig. 22) [221]. A BS pattern in the EEG during hypothermia after cardiac arrest is also associated with poor outcomes, especially if the bursts are identical [222].

Available studies investigating cEEG monitoring and outcomes have small sample sizes, lack external validation, are retrospective, and may be confounded by a self-fulfilling prophecy, as the decision to withdraw life-supporting therapy could be guided by combined information gathered from cEEG and clinical features. There is some evidence suggesting that cEEG can assist in identifying ICU patients with a favorable prognosis. In a comatose patient, recovery of an EEG towards continuous patterns within 12 h after cardiac arrest is strongly predictive of good outcomes [223]. EEG reactivity during hypothermia is likewise indicative of a good outcome [224].

There is little evidence concerning outcome prediction in noncardiac patients. In acute ischemic stroke, there is some evidence that qEEG in the subacute setting is of value for prognostication of functional status after six months [225]. In TBI, the absence of EEG reactivity is associated with poor outcomes (severe disability, vegetative status, or death), whereas EEG reactivity can be predictive of good outcomes [226]. In a study of 116 patients with poor-grade (Hunt and Hess score of 3 or lower) subarachnoid hemorrhage, Claassen et al. demonstrated that periodic discharges, NCSE, the absence of sleep architecture, and/or absent reactivity to external stimuli are associated with poor outcome [227].

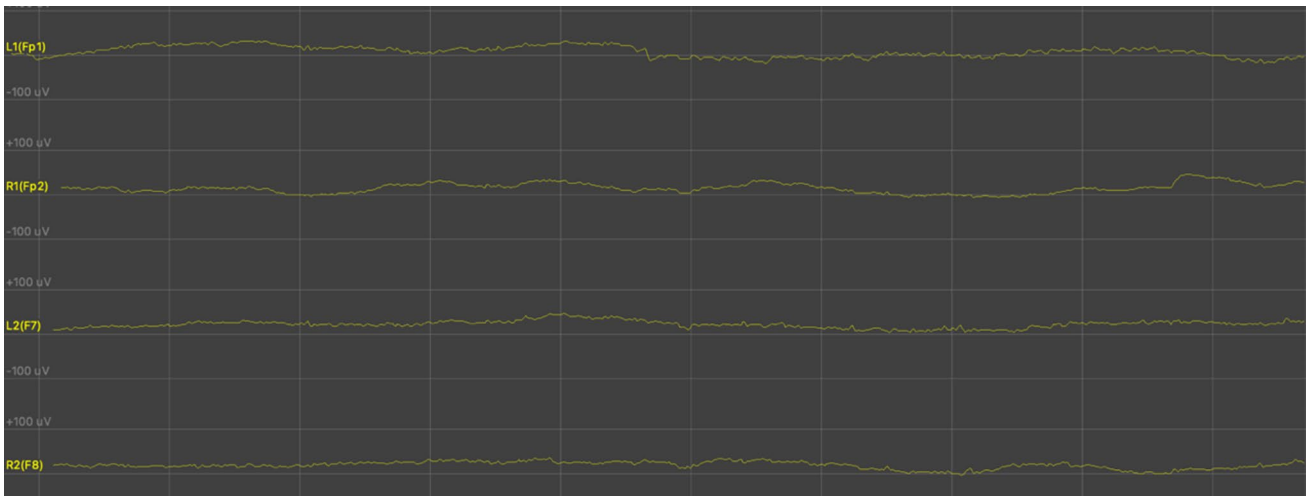

Fig. 22 Isoelectric electroencephalogram (Fp1-Fp2- F7- F8) of a 49-year-old patient admitted to the NeuroICU with an extensive intracerebral hemorrhage. Despite the emergent craniotomy, the patient had an unfavorable progression to brain death

1.12.7 Prediction and management of ICU delirium

Delirium is a prevalent clinical syndrome in both emergency departments and ICUs, with its occurrence strongly associated with patient age and the severity of underlying disease. The incidence of delirium in ICU patients has been reported to reach as high as 82%. Patients who develop delirium face increased risks of complications, mortality, cognitive impairment, prolonged hospitalization, and a higher likelihood of requiring institutional care after discharge [228]. Despite its high prevalence, delirium often remains underdiagnosed or inadequately documented by clinicians in the ICU setting.

To improve the identification of delirium, various assessment tools have been developed, including the Confusion Assessment Method (CAM), and its specific adaptation to ICU patients (CAM-ICU), the Nursing Delirium Screening Scale (Nu-DESC), and the Delirium Rating Scale (DRS). While these scales aid in the clinical identification of delirium and nd help distinguish it from other neurological disorders, the accurate identification of delirium remains time-consuming and challenging [228]. In this context, EEG monitoring, particularly qEEG, may serve as a valuable adjunct in identifying and assessing delirium. qEEG has shown promise in detecting delirium in ICU patients: an increase in delta power in frontal, central or temporal regions alone, or in combination with a reduction in beta frequencies in occipital regions showed a high sensitivity and specificity for delirium detection [229].

Robertson et al [229], identified several EEG biomarkers for delirium in mechanically ventilated ICU patients, using 24-h continuous EEG monitoring. Their study found that delta variability, high beta variability, relative theta power, and relative alpha power contributed independently to EEG-based identification of delirium or coma. Their findings provide a clear understanding of the neurophysiologic alterations associated with delirium and support the potential role of EEG in its detection and monitoring. In cases where deep sedation is required in ICU patients, clinicians are "blind" to the patient's neurological status or suggestive EEG pattern for delirium. However, studies have shown that comatose ICU patients who spend extended periods in burst suppression are more likely to develop post-coma delirium and experience prolonged recovery from it [230].

In summary, cEEG and qEEG provide additional information and should be considered explicitly in unclear prognostic situations [231]. The use of cEEG in the neuro-intensive care unit has become widespread over the last two decades. The Critical Care cEEG taskforce of the ACNS recommends its use for the detection of secondary injury in critically ill patients with altered mental status. The ACNS guidelines highlight its use for the diagnosis of nonconvulsive seizures and status epilepticus, as well as for the assessment of the efficacy of the treatment for these conditions. It also suggests conditions for appropriate use in the detection of secondary ischemia, evaluation of patients under pharmacological sedation, and prognostication of patients after cardiac arrest [232]. Unfortunately, technology and limited personnel limit the ability to provide cEEG. It requires live remote capabilities and an EEG technologist available to start, adjust, monitor, and interpret live EEG. It also requires the quick interpretation and storage of large amounts of data. Therefore, short-term (routine) EEG should be used to identify patterns at high risk for seizures and can help prioritize available resources or transfer patients to a higher level of care [233].

Finally, the use of qEEG appears to shorten the time it takes to review the EEG for seizure detection, although these results must be interpreted with caution and consideration of two key factors: first, a reduction in the EEG review time is not meaningful if the accuracy of the results is poor; second, although the initial response to compensate for the low accuracy of individual qEEG panels may be to review numerous panels along with select epochs of raw EEG, the overall review time may then increase, thereby undercutting the time-saving benefit. Thus, a delicate balance must exist among efficiency, accuracy, and practicality to allow qEEG to be useful. In practical terms, qEEG can serve as a complementary, valuable tool for portions of the cEEG that require more careful and detailed reading [234]. cEEG and short-term raw EEGs are required in critically ill patients with altered mental status. In patients on mechanical ventilation and receiving pharmacologic paralysis, qEEG is a helpful method of assuring that the patient is sufficiently sedated and unconscious. Continuous EEG and quantitative EEG provide additional information compared to spot EEG and should be specifically considered in unclear prognostic situations [231]. Following Gilmore's editorial discussing the original publication, cEEG may feel like a luxury, but it is necessary to improve patient care [235].

1.13 PART IV: Conclusion and learning points

Perioperative EEG monitoring is rooted in a robust physiological and neurobiological foundation, as it is intrinsically connected to cerebral metabolism and highly sensitive to common causes of cerebral injury. It enables the early detection of neuronal dysfunction at potentially reversible stages and identifies epileptic activity. This makes the EEG a powerful tool for providinga dynamic representation of brain function and offering real-time insights of the dose-dependent effects of anesthetic agents.

In contrast to generalized population-derived dosing rules and protocols, which do not account for individual pharmacokinetic and pharmacodynamic variability, perioperative EEG monitoring provides a more individualized approach

to assessing the impact of anesthetic drugs on the brain. It allows for more precise tailoring of anesthetic requirements to the specific needs of each patient, ensuring better outcomes and safer anesthesia management.

From a practical perspective, it is recommended to use EEG monitoring systems capable of recording multiple channels, displaying continuous raw EEG data, and offering DSA. These systems should also aloe for adjustments in EEG speed, voltage scale, and power scale of DSA. Additionally, the incorporation of other quantitative EEG parameters like the SEF, BSR, and EMG can further enhance the accuracy and utility of EEG monitoring in the perioperative setting..

Different groups and institutions have launched web-based platforms like ICETAP (www.icetap.org), Safe Brain Initiative (www. https://safebraininitiative.com) or https://eegforanesthesia.iars.org/ to advance education on perioperative applied electroencephalography. We strongly advocate the widespread adoption of comprehensive EEG monitoring during the perioperative period and in intensive care settings to enhance patient outcomes and brain health.

Supplementary Information The online version contains supplementary material available at https://doi.org/10.1007/s10877-024-01250-2.

Acknowledgements The authors would like to acknowledge Isabel Girão for the figure 1 and Nevena Mitic for the figure 5.

Author Contributions All the authors wrote, reviewed and approved the manuscript text. FAL prepared the Figs. 1, 2, 5, 7, 8, 9, 10, 11, 12, 13, 14, 15, 16, 17, 18, 19, 20, 21, 22. FN and AG prepared the Fig. 3 NM prepared the Fig. 4 MK prepared the Figs. 6, 9.

Funding The authors have not disclosed any funding.

Data availability No datasets were generated or analysed during the current study.

Declarations

Conflict of interest FAL is the Editor-in Chief of the Journal of Clinical Monitoring and Computing, CR is an Associate Editor of the Journal of Clinical Monitoring and Computing; MK and SV are members of the general board of editors of the Journal of Clinical Monitoring and Computing. None of them had interference with the Editorial process.

References

1. Brown EN, Lydic R, Schiff ND. General anesthesia, sleep, and coma. N Engl J Med. 2010;363(27):2638–50. https://doi.org/10.1056/NEJMra0808281.
2. Brown EN, Purdon PL, Van Dort CJ. General anesthesia and altered states of arousal: a systems neuroscience analysis. Annu Rev Neurosci. 2011;34:601–28. https://doi.org/10.1146/annurev-neuro-060909-153200.
3. Brown EN, Pavone KJ, Naranjo M. Multimodal general anesthesia: theory and practice. Anesth Analg. 2018;127(5):1246–58. https://doi.org/10.1213/ANE.0000000000003668.
4. Hudetz AG. General anesthesia and human brain connectivity. Brain Connect. 2012;2(6):291–302. https://doi.org/10.1089/brain.2012.0107.
5. Boveroux P, Vanhaudenhuyse A, Bruno MA, et al. Breakdown of within- and between-network resting state functional magnetic resonance imaging connectivity during propofol-induced loss of consciousness. Anesthesiology. 2010;113(5):1038–53. https://doi.org/10.1097/ALN.0b013e3181f697f5.
6. Guldenmund P, Demertzi A, Boveroux P, et al. Thalamus, brainstem and salience network connectivity changes during propofol-induced sedation and unconsciousness. Brain Connect. 2013;3(3):273–85. https://doi.org/10.1089/brain.2012.0117.
7. Lobo FA, Shander A. Modern anesthetic noninvasive monitoring: a deep look into perioperative care. J Cardiothorac Vasc Anesth. 2019;33(Suppl 1):S1-s2. https://doi.org/10.1053/j.jvca.2019.03.037.
8. Gutenberg eBook of The Notebooks of Leonardo Da Vinci. Accessed October 2024, https://www.gutenberg.org/cache/epub/5000/pg5000-images.html
9. Sandin RH, Enlund G, Samuelsson P, Lennmarken C. Awareness during anaesthesia: a prospective case study. Lancet. 2000;355(9205):707–11. https://doi.org/10.1016/s0140-6736(99)11010-9.
10. Rampil IJ. A primer for EEG signal processing in anesthesia. Anesthesiology. 1998;89(4):980–1002. https://doi.org/10.1097/00000542-199810000-00023.
11. Sigl JC, Chamoun NG. An introduction to bispectral analysis for the electroencephalogram. J Clin Monit. 1994;10(6):392–404. https://doi.org/10.1007/bf01618421.
12. Lobo FA, Saraiva AP, Nardiello I, Brandão J, Osborn IP. Electroencephalogram monitoring in anesthesia practice. Curr Anesthesiol Rep. 2021;11(3):169–80. https://doi.org/10.1007/s40140-021-00461-6.
13. Purdon PL, Sampson A, Pavone KJ, Brown EN. Clinical electroencephalography for anesthesiologists: Part I: background and basic signatures. Anesthesiology. 2015;123(4):937–60. https://doi.org/10.1097/ALN.0000000000000841.
14. Bennett C, Voss LJ, Barnard JP, Sleigh JW. Practical use of the raw electroencephalogram waveform during general anesthesia: the art and science. Anesth Analg. 2009;109(2):539–50. https://doi.org/10.1213/ane.0b013e3181a9fc38.
15. Chung CKE, Poon CCM, Irwin MG. Peri-operative neurological monitoring with electroencephalography and cerebral oximetry: a narrative review. Anaesthesia. 2022;77(Suppl 1):113–22. https://doi.org/10.1111/anae.15616.
16. Escallier KE, Nadelson MR, Zhou D, Avidan MS. Monitoring the brain: processed electroencephalogram and peri-operative outcomes. Anaesthesia. 2014;69(8):899–910. https://doi.org/10.1111/anae.12711.
17. Hight DF, Kaiser HA, Sleigh JW, Avidan MS. Continuing professional development module : An updated introduction to electroencephalogram-based brain monitoring during intended general anesthesia. *Can J Anaesth*. 2020;67(12):1858–1878 Module de développement professionnel continu : Une introduction mise à jour du monitorage cérébral par encéphalogramme pour une anesthésie générale planifiée. https://doi.org/10.1007/s12630-020-01820-3
18. Montupil J, Defresne A, Bonhomme V. The raw and processed electroencephalogram as a monitoring and diagnostic tool. J Cardiothorac Vasc Anesth. 2019;33(Suppl 1):S3-s10. https://doi.org/10.1053/j.jvca.2019.03.038.
19. Palanca BJ, Mashour GA, Avidan MS. Processed electroencephalogram in depth of anesthesia monitoring. Curr Opin

Anaesthesiol. 2009;22(5):553–9. https://doi.org/10.1097/ACO.0b013e3283304032.
20. Roche D, Mahon P. Depth of Anesthesia Monitoring. Anesthesiol Clin. 2021;39(3):477–92. https://doi.org/10.1016/j.anclin.2021.04.004.
21. Scheeren TWL, Kuizenga MH, Maurer H, Struys M, Heringlake M. Electroencephalography and brain oxygenation monitoring in the perioperative period. Anesth Analg. 2019;128(2):265–77. https://doi.org/10.1213/ane.0000000000002812.
22. Jameson LC, Sloan TB. Using EEG to monitor anesthesia drug effects during surgery. J Clin Monit Comput. 2006;20(6):445–72. https://doi.org/10.1007/s10877-006-9044-x.
23. Rasulo FA, Hopkins P, Lobo FA, et al. Processed electroencephalogram-based monitoring to guide sedation in critically Ill adult patients: recommendations from an international expert panel-based consensus. Neurocrit Care. 2023;38(2):296–311. https://doi.org/10.1007/s12028-022-01565-5.
24. Shander A, Lobel GP, Mathews DM. Brain monitoring and the depth of anesthesia: another goldilocks dilemma. Anesth Analg. 2018;126(2):705–9. https://doi.org/10.1213/ane.0000000000002383.
25. Aasheim A, Rosseland LA, Leonardsen AL, Romundstad L. Depth of anesthesia monitoring in Norway-a web-based survey. Acta Anaesthesiol Scand. 2024;68(6):781–7. https://doi.org/10.1111/aas.14420.
26. Coeckelenbergh S, Richebé P, Longrois D, Joosten A, De Hert S. Current trends in anesthetic depth and antinociception monitoring: an international survey. J Clin Monit Comput. 2022;36(5):1407–22. https://doi.org/10.1007/s10877-021-00781-2.
27. Moaiyeri Z, Mustafa J, Lamperti M, Lobo FA. Intraoperative use of processed electroencephalogram in a quaternary center: a quality improvement audit. J Clin Monit Comput. 2024. https://doi.org/10.1007/s10877-024-01189-4.
28. Pandit JJ, Cook TM, Jonker WR, O'Sullivan E. A national survey of anaesthetists (NAP5 Baseline) to estimate an annual incidence of accidental awareness during general anaesthesia in the UK. Anaesthesia. 2013;68(4):343–53. https://doi.org/10.1111/anae.12190.
29. Romagnoli S, Lobo FA, Picetti E, Rasulo FA, Robba C, Matta B. Non-invasive technology for brain monitoring: definition and meaning of the principal parameters for the International PRactice On TEChnology neuro-moniToring group (I-PROTECT). J Clin Monit Comput. 2024;38(4):827–45. https://doi.org/10.1007/s10877-024-01146-1.
30. Murakami S, Okada Y. Contributions of principal neocortical neurons to magnetoencephalography and electroencephalography signals. J Physiol. 2006;575(Pt 3):925–36. https://doi.org/10.1113/jphysiol.2006.105379.
31. Greenblatt AS, Beniczky S, Nascimento FA. Pitfalls in scalp EEG: Current obstacles and future directions. Epilepsy Behav. 2023;149:109500. https://doi.org/10.1016/j.yebeh.2023.109500.
32. Nayak CS AA. Publishing TIFS, ed. *EEG Normal Waveforms. [Updated 2023 Jul 24]*. 2024. https://www.ncbi.nlm.nih.gov/books/NBK539805/
33. Niedermeyer E, Schomer DL, da Silva FHL. *Niedermeyer's Electroencephalography: Basic Principles, Clinical Applications, and Related Fields*. Wolters Kluwer/Lippincott Williams & Wilkins Health; 2011.
34. Mecarelli O. *Clinical Electroencephalography*. Springer International Publishing; 2019.
35. Lopes da Silva F. Neural mechanisms underlying brain waves: from neural membranes to networks. Electroencephalogr Clin Neurophysiol. 1991;79(2):81–93. https://doi.org/10.1016/0013-4694(91)90044-5.
36. Herrmann CS, Strüber D, Helfrich RF, Engel AK. EEG oscillations: from correlation to causality. Int J Psychophysiol. 2016;103:12–21. https://doi.org/10.1016/j.ijpsycho.2015.02.003.
37. Fernandez LMJ, Lüthi A. Sleep Spindles: Mechanisms and Functions. Physiol Rev. 2020;100(2):805–68. https://doi.org/10.1152/physrev.00042.2018.
38. Wolter S, Friedel C, Böhler K, Hartmann U, Kox WJ, Hensel M. Presence of 14Hz spindle oscillations in the human EEG during deep anesthesia. Clin Neurophysiol. 2006;117(1):157–68. https://doi.org/10.1016/j.clinph.2005.08.031.
39. San-juan D, Chiappa KH, Cole AJ. Propofol and the electroencephalogram. Clin Neurophysiol. 2010;121(7):998–1006. https://doi.org/10.1016/j.clinph.2009.12.016.
40. Ching S, Cimenser A, Purdon PL, Brown EN, Kopell NJ. Thalamocortical model for a propofol-induced alpha-rhythm associated with loss of consciousness. Proc Natl Acad Sci U S A. 2010;107(52):22665–70. https://doi.org/10.1073/pnas.1017069108.
41. Ferenets R, Lipping T, Suominen P, et al. Comparison of the properties of EEG spindles in sleep and propofol anesthesia. Conf Proc IEEE Eng Med Biol Soc. 2006;2006:6356–9. https://doi.org/10.1109/iembs.2006.259909.
42. Huupponen E, Maksimow A, Lapinlampi P, et al. Electroencephalogram spindle activity during dexmedetomidine sedation and physiological sleep. Acta Anaesthesiol Scand. 2008;52(2):289–94. https://doi.org/10.1111/j.1399-6576.2007.01537.x.
43. Akeju O, Kim SE, Vazquez R, et al. Spatiotemporal dynamics of dexmedetomidine-induced electroencephalogram oscillations. PLoS ONE. 2016;11(10):e0163431. https://doi.org/10.1371/journal.pone.0163431.
44. Xi C, Sun S, Pan C, Ji F, Cui X, Li T. Different effects of propofol and dexmedetomidine sedation on electroencephalogram patterns: wakefulness, moderate sedation, deep sedation and recovery. PLoS ONE. 2018;13(6):e0199120. https://doi.org/10.1371/journal.pone.0199120.
45. Alshemeili M, Lobo FA. Is dexmedetomidine a lazy drug or do we have lazy anesthesiologists? Braz J Anesthesiol Mar-Apr. 2023;73(2):128–31. https://doi.org/10.1016/j.bjane.2023.01.001.
46. Akeju O, Pavone KJ, Westover MB, et al. A comparison of propofol- and dexmedetomidine-induced electroencephalogram dynamics using spectral and coherence analysis. Anesthesiology. 2014;121(5):978–89. https://doi.org/10.1097/ALN.0000000000000419.
47. Kilavik BE, Zaepffel M, Brovelli A, MacKay WA, Riehle A. The ups and downs of β oscillations in sensorimotor cortex. Exp Neurol. 2013;245:15–26. https://doi.org/10.1016/j.expneurol.2012.09.014.
48. Buzsáki G, Wang XJ. Mechanisms of gamma oscillations. Annu Rev Neurosci. 2012;35:203–25. https://doi.org/10.1146/annurev-neuro-062111-150444.
49. Goyal A, Miller J, Qasim SE, et al. Functionally distinct high and low theta oscillations in the human hippocampus. Nat Commun. 2020;11(1):2469. https://doi.org/10.1038/s41467-020-15670-6.
50. Zhang H, Watrous AJ, Patel A, Jacobs J. Theta and alpha oscillations are traveling waves in the human neocortex. Neuron. 2018;98(6):1269-81.e4. https://doi.org/10.1016/j.neuron.2018.05.019.
51. Bland BH, Oddie SD. Theta band oscillation and synchrony in the hippocampal formation and associated structures: the case for its role in sensorimotor integration. Behav Brain Res. 2001;127(1–2):119–36. https://doi.org/10.1016/s0166-4328(01)00358-8.
52. Pedemonte M, Goldstein-Daruech N, Velluti RA. Temporal correlations between heart rate, medullary units and hippocampal theta rhythm in anesthetized, sleeping and awake guinea pigs.

Auton Neurosci. 2003;107(2):99–104. https://doi.org/10.1016/s1566-0702(03)00132-2.
53. Knyazev GG. EEG delta oscillations as a correlate of basic homeostatic and motivational processes. Neurosci Biobehav Rev. 2012;36(1):677–95. https://doi.org/10.1016/j.neubiorev.2011.10.002.
54. Hirsch LJ, LaRoche SM, Gaspard N, et al. American clinical neurophysiology society's standardized critical care EEG terminology: 2012 version. J Clin Neurophysiol. 2013;30(1):1–27. https://doi.org/10.1097/WNP.0b013e3182784729.
55. Lobo FA, Vacas S, Rossetti AO, Robba C, Taccone FS. Does electroencephalographic burst suppression still play a role in the perioperative setting? Best Pract Res Clin Anaesthesiol. 2021;35(2):159–69. https://doi.org/10.1016/j.bpa.2020.10.007.
56. Siddiqi AZ, Froese L, Gomez A, et al. The effect of burst suppression on cerebral blood flow and autoregulation: a scoping review of the human and animal literature. Front Physiol. 2023;14:1204874. https://doi.org/10.3389/fphys.2023.1204874.
57. Buxton RB, Griffeth VE, Simon AB, Moradi F, Shmuel A. Variability of the coupling of blood flow and oxygen metabolism responses in the brain: a problem for interpreting BOLD studies but potentially a new window on the underlying neural activity. Front Neurosci. 2014;8:139. https://doi.org/10.3389/fnins.2014.00139.
58. Gur RC, Ragland JD, Reivich M, Greenberg JH, Alavi A, Gur RE. Regional differences in the coupling between resting cerebral blood flow and metabolism may indicate action preparedness as a default state. Cereb Cortex. 2009;19(2):375–82. https://doi.org/10.1093/cercor/bhn087.
59. Lewis LD, Ching S, Weiner VS, et al. Local cortical dynamics of burst suppression in the anaesthetized brain. Brain. 2013;136(Pt 9):2727–37. https://doi.org/10.1093/brain/awt174.
60. Fisch U, Jünger AL, Baumann SM, et al. Association between induced burst suppression and clinical outcomes in patients with refractory status epilepticus: a 9-year cohort study. Neurology. 2023;100(19):e1955-66. https://doi.org/10.1212/wnl.0000000000207129.
61. Klem GH, Lüders HO, Jasper HH, Elger C. The ten-twenty electrode system of the International Federation. The international federation of clinical neurophysiology. Electroencephalogr Clin Neurophysiol Suppl. 1999;52:3–6.
62. Seeck M, Koessler L, Bast T, et al. The standardized EEG electrode array of the IFCN. Clin Neurophysiol. 2017;128(10):2070–7. https://doi.org/10.1016/j.clinph.2017.06.254.
63. Kane N, Acharya J, Benickzy S, et al. A revised glossary of terms most commonly used by clinical electroencephalographers and updated proposal for the report format of the EEG findings. Revision 2017. Clin Neurophysiol Pract. 2017;2:170–85. https://doi.org/10.1016/j.cnp.2017.07.002.
64. Dubost C, Humbert P, Benizri A, Tourtier JP, Vayatis N, Vidal PP. Selection of the best electroencephalogram channel to predict the depth of anesthesia. Front Comput Neurosci. 2019;13:65. https://doi.org/10.3389/fncom.2019.00065.
65. Yasir KA, Liu WM. Social distancing mediated generalized model to predict epidemic spread of COVID-19. Nonlinear Dyn. 2021;106(2):1187–95. https://doi.org/10.1007/s11071-021-06424-0.
66. Ahn S, Rubchinsky LL. Short desynchronization episodes prevail in synchronous dynamics of human brain rhythms. Chaos. 2013;23(1):013138. https://doi.org/10.1063/1.4794793.
67. Jiang D, Lu Y-n, Ma Y, Wang Y. Robust sleep stage classification with single-channel EEG signals using multimodal decomposition and HMM-based refinement. Expert Syst Appl. 2019;121:188–203. https://doi.org/10.1016/j.eswa.2018.12.023.
68. Geering BA, Achermann P, Eggimann F, Borbély AA. Period-amplitude analysis and power spectral analysis: a comparison based on all-night sleep EEG recordings. J Sleep Res. 1993;2(3):121–9. https://doi.org/10.1111/j.1365-2869.1993.tb00074.x.
69. Diniz RC, Fontenele AMM, Carmo L, et al. Quantitative methods in electroencephalography to access therapeutic response. Biomed Pharmacother. 2016;81:182–91. https://doi.org/10.1016/j.biopha.2016.02.046.
70. Sleigh JW. Depth of anesthesia: perhaps the patient isn't a submarine. Anesthesiology. 2011;115(6):1149–50. https://doi.org/10.1097/ALN.0b013e3182390396.
71. Lobo FA, Schraag S. Limitations of anaesthesia depth monitoring. Curr Opin Anaesthesiol. 2011;24(6):657–64. https://doi.org/10.1097/ACO.0b013e32834c7aba.
72. Obert DP, Schneider F, Schneider G, et al. Performance of the SEDLine monitor: Age dependency and time delay. Anesth Analg. 2023;137(4):887–95. https://doi.org/10.1213/ane.0000000000006369.
73. Lichtenfeld F, Kratzer S, Hinzmann D, García PS, Schneider G, Kreuzer M. The influence of electromyographic on electroencephalogram-based monitoring: putting the forearm on the forehead. Anesth Analg. 2024;138(6):1285–94. https://doi.org/10.1213/ane.0000000000006652.
74. Dahaba AA. Different conditions that could result in the bispectral index indicating an incorrect hypnotic state. Anesth Analg. 2005;101(3):765–73. https://doi.org/10.1213/01.ane.0000167269.62966.af.
75. Hajat Z, Ahmad N, Andrzejowski J. The role and limitations of EEG-based depth of anaesthesia monitoring in theatres and intensive care. Anaesthesia. 2017;72(Suppl 1):38–47. https://doi.org/10.1111/anae.13739.
76. Thedim M, Vacas S. *Multimodal monitoring*. In Lobo & Lamperti, Textbook of Perioperative Brain Monitoring. Springer Nature; 2025 *in press*.
77. Viertiö-Oja H, Maja V, Särkelä M, et al. Description of the entropy algorithm as applied in the Datex-Ohmeda S/5 entropy module. Acta Anaesthesiol Scand. 2004;48(2):154–61. https://doi.org/10.1111/j.0001-5172.2004.00322.x.
78. Ebensperger M, Kreuzer M, Kratzer S, Schneider G, Schwerin S. Continuity with caveats in anesthesia: state and response entropy of the EEG. J Clin Monit Comput. 2024;38(5):1057–68. https://doi.org/10.1007/s10877-024-01130-9.
79. Georgii MT, Pilge S, Schneider G, Kreuzer M. State entropy and burst suppression ratio can show contradictory information: a retrospective study. Eur J Anaesthesiol. 2020;37(12):1084–92. https://doi.org/10.1097/eja.0000000000001312.
80. Shalbaf R, Behnam H, Sleigh JW, Steyn-Ross A, Voss LJ. Monitoring the depth of anesthesia using entropy features and an artificial neural network. J Neurosci Methods. 2013;218(1):17–24. https://doi.org/10.1016/j.jneumeth.2013.03.008.
81. Loomis AL, Harvey EN, Hobart GA. Cerebral states during sleep, as studied by human brain potentials. J Exp Psychol. 1937;21(2):127–44. https://doi.org/10.1037/h0057431.
82. Kreuer S, Biedler A, Larsen R, Schoth S, Altmann S, Wilhelm W. The Narcotrend–a new EEG monitor designed to measure the depth of anaesthesia. A comparison with bispectral index monitoring during propofol-remifentanil-anaesthesia. Anaesthesist. 2001;50(12):921–5. https://doi.org/10.1007/s00101-001-0242-0.
83. Kreuer S, Wilhelm W. The Narcotrend monitor. Best Pract Res Clin Anaesthesiol. 2006;20(1):111–9. https://doi.org/10.1016/j.bpa.2005.08.010.
84. Drover D, Ortega HR. Patient state index. Best Pract Res Clin Anaesthesiol. 2006;20(1):121–8. https://doi.org/10.1016/j.bpa.2005.07.008.

85. Jensen EW, Valencia JF, López A, et al. Monitoring hypnotic effect and nociception with two EEG-derived indices, qCON and qNOX, during general anaesthesia. Acta Anaesthesiol Scand. 2014;58(8):933–41. https://doi.org/10.1111/aas.12359.
86. Melia U, Gabarron E, Agustí M, et al. Comparison of the qCON and qNOX indices for the assessment of unconsciousness level and noxious stimulation response during surgery. J Clin Monit Comput. 2017;31(6):1273–81. https://doi.org/10.1007/s10877-016-9948-z.
87. Melia U, Vallverdú M, Borrat X, et al. Prediction of Nociceptive Responses during Sedation by Linear and Non-Linear Measures of EEG Signals in High Frequencies. PLoS ONE. 2015;10(4):e0123464. https://doi.org/10.1371/journal.pone.0123464.
88. Zikov T, Bibian S, Dumont GA, Huzmezan M, Ries CR. Quantifying cortical activity during general anesthesia using wavelet analysis. IEEE Trans Biomed Eng. 2006;53(4):617–32. https://doi.org/10.1109/tbme.2006.870255.
89. West N, McBeth PB, Brodie SM, et al. Feasibility of continuous sedation monitoring in critically ill intensive care unit patients using the NeuroSENSE WAV(CNS) index. J Clin Monit Comput. 2018;32(6):1081–91. https://doi.org/10.1007/s10877-018-0115-6.
90. Görges M, West NC, Cooke EM, et al. Evaluating NeuroSENSE for assessing depth of hypnosis during desflurane anesthesia: an adaptive, randomized-controlled trial. *Can J Anaesth*. Mar 2020;67(3):324–335 Une évaluation du moniteur NeuroSENSE pour mesurer la profondeur de l'hypnose pendant une anesthésie au desflurane : une étude randomisée contrôlée adaptable. https://doi.org/10.1007/s12630-019-01522-5
91. Ojha P. Berger and the breakthrough: a centennial celebration of the human electroencephalogram. Neurodiagn J. 2024;64(2):69–74. https://doi.org/10.1080/21646821.2024.2327268.
92. Gibbs FAGE. Lennox WG Effect on the electroencephalogram of certain drugs which influence nervous activity. Arch Intern Med (Chic). 1937;60(1):154–66.
93. Thomsen KK, Sessler DI, Krause L, et al. Processed electroencephalography-guided general anesthesia and norepinephrine requirements: a randomized trial in patients having vascular surgery. J Clin Anesth. 2024;95:111459. https://doi.org/10.1016/j.jclinane.2024.111459.
94. Chiang MH, Wu SC, Hsu SW, Chin JC. Bispectral Index and non-Bispectral Index anesthetic protocols on postoperative recovery outcomes. Minerva Anestesiol. 2018;84(2):216–28. https://doi.org/10.23736/s0375-9393.17.12033-x.
95. Lewis SR, Pritchard MW, Fawcett LJ, Punjasawadwong Y. Bispectral index for improving intraoperative awareness and early postoperative recovery in adults. Cochrane Database Syst Rev. 2019. https://doi.org/10.1002/14651858.CD003843.pub4.
96. Foreman B, Claassen J. Quantitative EEG for the detection of brain ischemia. Crit Care. 2012;16(2):216. https://doi.org/10.1186/cc11230.
97. Gitti N, Renzi S, Marchesi M, et al. Seeking the light in intensive care unit sedation: the optimal sedation strategy for critically Ill patients. Front Med (Lausanne). 2022;9:901343. https://doi.org/10.3389/fmed.2022.901343.
98. Thedim M, Vacas S. Postoperative delirium and the older adult: untangling the confusion. J Neurosurg Anesthesiol. 2024;36(3):184–9. https://doi.org/10.1097/ana.0000000000000971.
99. Song X, Roy B, Vacas S, et al. Brain regional homogeneity changes after short-term positive airway pressure treatment in patients with obstructive sleep apnea. Sleep Med. 2022;91:12–20. https://doi.org/10.1016/j.sleep.2022.02.005.
100. Vacas S, Cole DJ, Cannesson M. Cognitive decline associated with anesthesia and surgery in older patients. JAMA. 2021. https://doi.org/10.1001/jama.2021.4773.
101. Thedim M, Aydin D, Schneider G, Kumar R, Kreuzer M, Vacas S. Preoperative biomarkers associated with delayed neurocognitive recovery. J Clin Monit and Comput. 2024. https://doi.org/10.1007/s10877-024-01218-2.
102. Vacas S, Canales C, Deiner SG, Cole DJ. Perioperative brain health in the older adult: a patient safety imperative. Anesth Analg. 2022;135(2):316–28. https://doi.org/10.1213/ANE.0000000000006090.
103. Jin Z, Hu J, Ma D. Postoperative delirium: perioperative assessment, risk reduction, and management. Br J Anaesth. 2020;125(4):492–504. https://doi.org/10.1016/j.bja.2020.06.063.
104. Bocskai T, Kovács M, Szakács Z, et al. Is the bispectral index monitoring protective against postoperative cognitive decline? A systematic review with meta-analysis. PLoS ONE. 2020;15(2):e0229018. https://doi.org/10.1371/journal.pone.0229018.
105. MacKenzie KK, Britt-Spells AM, Sands LP, Leung JM. Processed electroencephalogram monitoring and postoperative delirium: a systematic review and meta-analysis. Anesthesiology. 2018;129(3):417–27. https://doi.org/10.1097/aln.0000000000002323.
106. Wildes TS, Mickle AM, Ben Abdallah A, et al. Effect of electroencephalography-guided anesthetic administration on postoperative delirium among older adults undergoing major surgery: the ENGAGES randomized clinical trial. JAMA. 2019;321(5):473–83. https://doi.org/10.1001/jama.2018.22005.
107. Li J, Shalabi A, Ji F, Meng L. Monitoring cerebral ischemia during carotid endarterectomy and stenting. J Biomed Res. 2017;31(1):11–6. https://doi.org/10.7555/jbr.31.20150171.
108. Woodworth GF, McGirt MJ, Than KD, Huang J, Perler BA, Tamargo RJ. 2007 Selective versus routine intraoperative shunting during carotid endarterectomy: a multivariate outcome analysis. *Neurosurgery*. 61(6):1170–6; discussion 1176–7. https://doi.org/10.1227/01.neu.0000306094.15270.40
109. Zorrilla-Vaca A, Healy RJ, Wu CL, Grant MC. Relation between bispectral index measurements of anesthetic depth and postoperative mortality: a meta-analysis of observational studies. *Can J Anaesth*. Jun 2017;64(6):597–607. Relation entre les mesures de l'indice bispectral de profondeur de l'anesthésie et la mortalité postopératoire: méta-analyse des études observationnelles. https://doi.org/10.1007/s12630-017-0872-6
110. Willingham M, Ben Abdallah A, Gradwohl S, et al. Association between intraoperative electroencephalographic suppression and postoperative mortality. Br J Anaesth. 2014;113(6):1001–8. https://doi.org/10.1093/bja/aeu105.
111. Li Y, Bohringer C, Liu H. Double standard: why electrocardiogram is standard care while electroencephalogram is not? Curr Opin Anaesthesiol. 2020;33(5):626–32. https://doi.org/10.1097/aco.0000000000000902.
112. Yang Q, Zhou F, Li A, Dong H. Neural substrates for the regulation of sleep and general anesthesia. Curr Neuropharmacol. 2022;20(1):72–84. https://doi.org/10.2174/1570159x19666211214144639.
113. Jiang-Xie LF, Yin L, Zhao S, et al. A Common neuroendocrine substrate for diverse general anesthetics and sleep. Neuron. 2019;102(5):1053-65.e4. https://doi.org/10.1016/j.neuron.2019.03.033.
114. Casey CP, Tanabe S, Farahbakhsh Z, et al. Distinct EEG signatures differentiate unconsciousness and disconnection during anaesthesia and sleep. Br J Anaesth. 2022;128(6):1006–18. https://doi.org/10.1016/j.bja.2022.01.010.

115. McCarthy MM, Brown EN, Kopell N. Potential network mechanisms mediating electroencephalographic beta rhythm changes during propofol-induced paradoxical excitation. J Neurosci. 2008;28(50):13488–504. https://doi.org/10.1523/jneurosci.3536-08.2008.
116. Purdon PL, Pierce ET, Mukamel EA, et al. Electroencephalogram signatures of loss and recovery of consciousness from propofol. Proc Natl Acad Sci U S A. 2013;110(12):E1142-51. https://doi.org/10.1073/pnas.1221180110.
117. Gaskell AL, Hight DF, Winders J, et al. Frontal alpha-delta EEG does not preclude volitional response during anaesthesia: prospective cohort study of the isolated forearm technique. Br J Anaesth. 2017;119(4):664–73. https://doi.org/10.1093/bja/aex170.
118. Akrawi WP, Drummond JC, Kalkman CJ, Patel PM. A comparison of the electrophysiologic characteristics of EEG burst-suppression as produced by isoflurane, thiopental, etomidate, and propofol. J Neurosurg Anesthesiol. 1996;8(1):40–6. https://doi.org/10.1097/00008506-199601000-00010.
119. Besch G, Liu N, Samain E, et al. Occurrence of and risk factors for electroencephalogram burst suppression during propofol-remifentanil anaesthesia. Br J Anaesth. 2011;107(5):749–56. https://doi.org/10.1093/bja/aer235.
120. Pilge S, Jordan D, Kreuzer M, Kochs EF, Schneider G. Burst suppression-MAC and burst suppression-CP_{50} as measures of cerebral effects of anaesthetics. Br J Anaesth. 2014;112(6):1067–74. https://doi.org/10.1093/bja/aeu016.
121. Touchard C, Cartailler J, Levé C, et al. EEG power spectral density under Propofol and its association with burst suppression, a marker of cerebral fragility. Clin Neurophysiol. 2019;130(8):1311–9. https://doi.org/10.1016/j.clinph.2019.05.014.
122. Franks NP. General anaesthesia: from molecular targets to neuronal pathways of sleep and arousal. Nat Rev Neurosci. 2008;9(5):370–86. https://doi.org/10.1038/nrn2372.
123. Akeju O, Westover MB, Pavone KJ, et al. Effects of sevoflurane and propofol on frontal electroencephalogram power and coherence. Anesthesiology. 2014;121(5):990–8. https://doi.org/10.1097/aln.0000000000000436.
124. Pavone KJ, Su L, Gao L, et al. Lack of responsiveness during the onset and offset of sevoflurane anesthesia is associated with decreased awake-alpha oscillation power. Front Syst Neurosci. 2017;11:38. https://doi.org/10.3389/fnsys.2017.00038.
125. Chamadia S, Pedemonte JC, Hahm EY, et al. Delta oscillations phase limit neural activity during sevoflurane anesthesia. Commun Biol. 2019;2:415. https://doi.org/10.1038/s42003-019-0664-3.
126. Putzke C, Hanley PJ, Schlichthörl G, et al. Differential effects of volatile and intravenous anesthetics on the activity of human TASK-1. Am J Physiol Cell Physiol. 2007;293(4):C1319-26. https://doi.org/10.1152/ajpcell.00100.2007.
127. Kindler CH, Pietruck C, Yost CS, Sampson ER, Gray AT. Localization of the tandem pore domain K+ channel TASK-1 in the rat central nervous system. Brain Res Mol Brain Res. 2000;80(1):99–108. https://doi.org/10.1016/s0169-328x(00)00136-4.
128. Dahal R, Tamura K, Pan DS, et al. Effect of sevoflurane anesthesia on intraoperative spikes, high-frequency oscillations, and phase-amplitude coupling in mri-normal hippocampus. J Clin Neurophysiol. 2023. https://doi.org/10.1097/wnp.0000000000001031.
129. Lee U, Ku S, Noh G, Baek S, Choi B, Mashour GA. Disruption of frontal-parietal communication by ketamine, propofol, and sevoflurane. Anesthesiology. 2013;118(6):1264–75. https://doi.org/10.1097/ALN.0b013e31829103f5.
130. de la Salle S, Choueiry J, Shah D, et al. Effects of ketamine on resting-state EEG activity and their relationship to perceptual/dissociative symptoms in healthy humans. Front Pharmacol. 2016;7:348. https://doi.org/10.3389/fphar.2016.00348.
131. Vlisides PE, Bel-Bahar T, Lee U, et al. Neurophysiologic correlates of ketamine sedation and anesthesia: a high-density electroencephalography study in healthy volunteers. Anesthesiology. 2017;127(1):58–69. https://doi.org/10.1097/aln.0000000000001671.
132. Blain-Moraes S, Lee U, Ku S, Noh G, Mashour GA. Electroencephalographic effects of ketamine on power, cross-frequency coupling, and connectivity in the alpha bandwidth. Front Syst Neurosci. 2014;8:114. https://doi.org/10.3389/fnsys.2014.00114.
133. Akeju O, Song AH, Hamilos AE, et al. Electroencephalogram signatures of ketamine anesthesia-induced unconsciousness. Clin Neurophysiol. 2016;127(6):2414–22. https://doi.org/10.1016/j.clinph.2016.03.005.
134. Liu T, Zhang X, Li A, et al. Effects of intra-operative administration of subanesthetic s-ketamine on emergence from sevoflurane anesthesia: a randomized double-blind placebo-controlled study. BMC Anesthesiol. 2023;23(1):221. https://doi.org/10.1186/s12871-023-02170-5.
135. Barreto Chang OL, Kreuzer M, Morgen DF, Possin KL, García PS. Ketamine-associated intraoperative electroencephalographic signatures of elderly patients with and without preoperative cognitive impairment. Anesth Analg. 2022;135(4):683–92. https://doi.org/10.1213/ane.0000000000005875.
136. Hirota K, Kubota T, Ishihara H, Matsuki A. The effects of nitrous oxide and ketamine on the bispectral index and 95% spectral edge frequency during propofol-fentanyl anaesthesia. Eur J Anaesthesiol. 1999;16(11):779–83. https://doi.org/10.1046/j.1365-2346.1999.00585.x.
137. Maksimow A, Särkelä M, Långsjö JW, et al. Increase in high frequency EEG activity explains the poor performance of EEG spectral entropy monitor during S-ketamine anesthesia. Clin Neurophysiol. 2006;117(8):1660–8. https://doi.org/10.1016/j.clinph.2006.05.011.
138. Vereecke HE, Vanluchene AL, Mortier EP, Everaert K, Struys MM. The effects of ketamine and rocuronium on the A-Line auditory evoked potential index, bispectral index, and spectral entropy monitor during steady state propofol and remifentanil anesthesia. Anesthesiology. 2006;105(6):1122–34. https://doi.org/10.1097/00000542-200612000-00012.
139. van Heusden K, Cooke E, Brodie S, et al. Effect of ketamine on the NeuroSENSE WAV(CNS) during propofol anesthesia; a randomized feasibility trial. J Clin Monit Comput. 2021;35(3):557–67. https://doi.org/10.1007/s10877-020-00511-0.
140. Faraoni D, Salengros JC, Engelman E, Ickx B, Barvais L. Ketamine has no effect on bispectral index during stable propofol-remifentanil anaesthesia. Br J Anaesth. 2009;102(3):336–9. https://doi.org/10.1093/bja/aen403.
141. Berti M, Baciarello M, Troglio R, Fanelli G. Clinical uses of low-dose ketamine in patients undergoing surgery. Curr Drug Targets. 2009;10(8):707–15. https://doi.org/10.2174/138945009788982496.
142. Tucker AP, Kim YI, Nadeson R, Goodchild CS. Investigation of the potentiation of the analgesic effects of fentanyl by ketamine in humans: a double-blinded, randomised, placebo controlled, crossover study of experimental pain[ISRCTN83088383]. BMC Anesthesiol. 2005. https://doi.org/10.1186/1471-2253-5-2.
143. Herd DW, Anderson BJ, Keene NA, Holford NH. Investigating the pharmacodynamics of ketamine in children. Paediatr Anaesth. 2008;18(1):36–42. https://doi.org/10.1111/j.1460-9592.2007.02384.x.
144. Martini C, Olofsen E, Yassen A, Aarts L, Dahan A. Pharmacokinetic-pharmacodynamic modeling in acute and chronic pain: an

overview of the recent literature. Expert Rev Clin Pharmacol. 2011;4(6):719–28. https://doi.org/10.1586/ecp.11.59.
145. Flores FJ, Ching S, Hartnack K, et al. A PK-PD model of ketamine-induced high-frequency oscillations. J Neural Eng. 2015;12(5):056006. https://doi.org/10.1088/1741-2560/12/5/056006.
146. Willetts J, Rice A, Balster RL. (+)-N-Allylnormetazocine (NANM)-like discriminative stimulus effects of N-methyl-D-aspartate (NMDA) antagonists. Behav Pharmacol. 1990;1(5):453–8.
147. Nelson LE, Lu J, Guo T, Saper CB, Franks NP, Maze M. The alpha2-adrenoceptor agonist dexmedetomidine converges on an endogenous sleep-promoting pathway to exert its sedative effects. Anesthesiology. 2003;98(2):428–36. https://doi.org/10.1097/00000542-200302000-00024.
148. Khasar SG, Green PG, Chou B, Levine JD. Peripheral nociceptive effects of alpha 2-adrenergic receptor agonists in the rat. Neuroscience. 1995;66(2):427–32. https://doi.org/10.1016/0306-4522(94)00562-j.
149. Grewal A. Dexmedetomidine: New avenues. J Anaesthesiol Clin Pharmacol. 2011;27(3):297–302. https://doi.org/10.4103/0970-9185.83670.
150. Liang F, Liu M, Fu X, Zhou X, Chen P, Han F. Dexmedetomidine attenuates neuropathic pain in chronic constriction injury by suppressing NR2B, NF-κB, and iNOS activation. Saudi Pharm J. 2017;25(4):649–54. https://doi.org/10.1016/j.jsps.2017.04.039.
151. Zhang L, Fang K, Tao S, et al. Electroencephalography-demonstrated mechanisms of dexmedetomidine-mediated deepening of propofol anesthesia: an observational study. Perioper Med (Lond). 2021;10(1):44. https://doi.org/10.1186/s13741-021-00213-4.
152. Vacas S, Maze M. Can sedation fulfill the physiological role of sleep? *Handbook on Burnout and Sleep Deprivation: Risk Factors, Management Strategies and Impact on Performance and Behavior*. 2015;
153. Vacas S, Kurien P, Maze M. Sleep and anesthesia - common mechanisms of action. Sleep Med Clin. 2013;8(1):1–9. https://doi.org/10.1016/j.jsmc.2012.11.009.
154. Malver LP, Brokjaer A, Staahl C, Graversen C, Andresen T, Drewes AM. Electroencephalography and analgesics. Br J Clin Pharmacol. 2014;77(1):72–95. https://doi.org/10.1111/bcp.12137.
155. Lersch F, Correia PC, Hight D, Kaiser HA, Berger-Estilita J. The nuts and bolts of multimodal anaesthesia in the 21st century: a primer for clinicians. Curr Opin Anaesthesiol. 2023;36(6):666–75. https://doi.org/10.1097/aco.0000000000001308.
156. Noh GJ, Kim KM, Jeong YB, et al. Electroencephalographic approximate entropy changes in healthy volunteers during remifentanil infusion. Anesthesiology. 2006;104(5):921–32. https://doi.org/10.1097/00000542-200605000-00006.
157. Egan TD, Minto CF, Hermann DJ, Barr J, Muir KT, Shafer SL. Remifentanil versus alfentanil: comparative pharmacokinetics and pharmacodynamics in healthy adult male volunteers. Anesthesiology. 1996;84(4):821–33. https://doi.org/10.1097/00000542-199604000-00009.
158. Balanza GA, Bharadwaj KM, Mullen AC, et al. An electroencephalogram biomarker of fentanyl drug effects. PNAS Nexus. 2022. https://doi.org/10.1093/pnasnexus/pgac158.
159. Minto CF, Schnider TW, Egan TD, et al. Influence of age and gender on the pharmacokinetics and pharmacodynamics of remifentanil. I Model dev Anesthesiol. 1997;86(1):10–23. https://doi.org/10.1097/00000542-199701000-00004.
160. Khodayari-Rostamabad A, Graversen C, Malver LP, et al. A cortical source localization analysis of resting EEG data after remifentanil infusion. Clin Neurophysiol. 2015;126(5):898–905. https://doi.org/10.1016/j.clinph.2014.08.006.
161. Ferreira DA, Nunes CS, Antunes LM, et al. The effect of a remifentanil bolus on the bispectral index of the EEG (BIS) in anaesthetized patients independently from intubation and surgical stimuli. Eur J Anaesthesiol. 2006;23(4):305–10. https://doi.org/10.1017/s0265021505001997.
162. Apkarian AV, Bushnell MC, Treede RD, Zubieta JK. Human brain mechanisms of pain perception and regulation in health and disease. Eur J Pain. 2005;9(4):463–84. https://doi.org/10.1016/j.ejpain.2004.11.001.
163. Mouraux A, Iannetti GD. The search for pain biomarkers in the human brain. Brain. 2018;141(12):3290–307. https://doi.org/10.1093/brain/awy281.
164. Pujol J, Martínez-Vilavella G, Gallart L, et al. Effects of remifentanil on brain responses to noxious stimuli during deep propofol sedation. Br J Anaesth. 2023;130(2):e330-8. https://doi.org/10.1016/j.bja.2022.06.038.
165. Ploner M, Sorg C, Gross J. Brain rhythms of pain. Trends Cogn Sci. 2017;21(2):100–10. https://doi.org/10.1016/j.tics.2016.12.001.
166. Aho AJ, Lyytikäinen LP, Yli-Hankala A, Kamata K, Jäntti V. Explaining Entropy responses after a noxious stimulus, with or without neuromuscular blocking agents, by means of the raw electroencephalographic and electromyographic characteristics. Br J Anaesth. 2011;106(1):69–76. https://doi.org/10.1093/bja/aeq300.
167. Bischoff P, Kochs E, Haferkorn D, am Esch SJ. Intraoperative EEG changes in relation to the surgical procedure during isoflurane-nitrous oxide anesthesia: hysterectomy versus mastectomy. J Clin Anesth. 1996;8(1):36–43. https://doi.org/10.1016/0952-8180(95)00170-0.
168. García PS, Kreuzer M, Hight D, Sleigh JW. Effects of noxious stimulation on the electroencephalogram during general anaesthesia: a narrative review and approach to analgesic titration. Br J Anaesth. 2021;126(2):445–57. https://doi.org/10.1016/j.bja.2020.10.036.
169. Hagihira S, Takashina M, Mori T, Ueyama H, Mashimo T. Electroencephalographic bicoherence is sensitive to noxious stimuli during isoflurane or sevoflurane anesthesia. Anesthesiology. 2004;100(4):818–25. https://doi.org/10.1097/00000542-200404000-00011.
170. Hight DF, Gaskell AL, Kreuzer M, Voss LJ, García PS, Sleigh JW. Transient electroencephalographic alpha power loss during maintenance of general anaesthesia. Br J Anaesth. 2019;122(5):635–42. https://doi.org/10.1016/j.bja.2018.11.029.
171. Kaada BR, Thomas F, Alnaes E, Wester K. EEG synchronization induced by high frequency midbrain reticular stimulation in anesthetized cats. Electroencephalogr Clin Neurophysiol. 1967;22(3):220–30. https://doi.org/10.1016/0013-4694(67)90224-6.
172. Litscher G, Schwarz G. Is there paradoxical arousal reaction in the EEG subdelta range in patients during anesthesia? J Neurosurg Anesthesiol. 1999;11(1):49–52. https://doi.org/10.1097/00008506-199901000-00010.
173. Sleigh JW, Leslie K, Voss L. The effect of skin incision on the electroencephalogram during general anesthesia maintained with propofol or desflurane. J Clin Monit Comput. 2010;24(4):307–18. https://doi.org/10.1007/s10877-010-9251-3.
174. Wilder-Smith OH, Hagon O, Tassonyi E. EEG arousal during laryngoscopy and intubation: comparison of thiopentone or propofol supplemented with nitrous oxide. Br J Anaesth. 1995;75(4):441–6. https://doi.org/10.1093/bja/75.4.441.
175. Ledowski T. Objective monitoring of nociception: a review of current commercial solutions. Br J Anaesth. 2019;123(2):e312-21. https://doi.org/10.1016/j.bja.2019.03.024.

176. De Jonckheere J, Bonhomme V, Jeanne M, et al. Physiological signal processing for individualized anti-nociception management during general anesthesia: a review. Yearb Med Inform. 2015;10(1):95–101. https://doi.org/10.15265/iy-2015-004.
177. Moaiyeri Z, Duarte F, Lamperti M, Lobo FA. Peri-operative multimodal monitoring: a real need or a luxury? J Clin Monit Comput. 2023;37(2):709–14. https://doi.org/10.1007/s10877-022-00914-1.
178. Yang S, Xiao W, Wu H, et al. Management based on multimodal brain monitoring may improve functional connectivity and postoperative neurocognition in elderly patients undergoing spinal surgery. Front Aging Neurosci. 2021;13:705287. https://doi.org/10.3389/fnagi.2021.705287.
179. Rossini PM, Rossi S, Babiloni C, Polich J. Clinical neurophysiology of aging brain: from normal aging to neurodegeneration. Prog Neurobiol. 2007;83(6):375–400. https://doi.org/10.1016/j.pneurobio.2007.07.010.
180. Giaquinto S, Nolfe G. The EEG in the normal elderly: a contribution to the interpretation of aging and dementia. Electroencephalogr Clin Neurophysiol. 1986;63(6):540–6. https://doi.org/10.1016/0013-4694(86)90141-0.
181. Badke D'Andrea C, Marek S, Van AN, et al. Thalamo-cortical and cerebello-cortical functional connectivity in development. Cereb Cortex. 2023;33(15):9250–62. https://doi.org/10.1093/cercor/bhad198.
182. Lee J, Kim HJ. Normal aging induces changes in the brain and neurodegeneration progress: review of the structural, biochemical, metabolic, cellular, and molecular changes. Front Aging Neurosci. 2022;14:931536. https://doi.org/10.3389/fnagi.2022.931536.
183. Cornelissen L, Kim SE, Purdon PL, Brown EN, Berde CB. Age-dependent electroencephalogram (EEG) patterns during sevoflurane general anesthesia in infants. Elife. 2015;4:e06513. https://doi.org/10.7554/eLife.06513.
184. Akeju O, Pavone KJ, Thum JA, et al. Age-dependency of sevoflurane-induced electroencephalogram dynamics in children. Br J Anaesth. 2015;115:i66-76. https://doi.org/10.1093/bja/aev114.
185. Cornelissen L, Kim SE, Lee JM, Brown EN, Purdon PL, Berde CB. Electroencephalographic markers of brain development during sevoflurane anaesthesia in children up to 3 years old. Br J Anaesth. 2018;120(6):1274–86. https://doi.org/10.1016/j.bja.2018.01.037.
186. Bong CL, Balanza GA, Khoo CE, Tan JS, Desel T, Purdon PL. A narrative review illustrating the clinical utility of electroencephalogram-guided anesthesia care in children. Anesth Analg. 2023;137(1):108–23. https://doi.org/10.1213/ane.0000000000006267.
187. Lee JM, Akeju O, Terzakis K, et al. A Prospective Study of Age-dependent Changes in Propofol-induced Electroencephalogram Oscillations in Children. Anesthesiology. 2017;127(2):293–306. https://doi.org/10.1097/aln.0000000000001717.
188. Gao W, Alcauter S, Smith JK, Gilmore JH, Lin W. Development of human brain cortical network architecture during infancy. Brain Struct Funct. 2015;220(2):1173–86. https://doi.org/10.1007/s00429-014-0710-3.
189. Alcauter S, Lin W, Smith JK, et al. Development of thalamocortical connectivity during infancy and its cognitive correlations. J Neurosci. 2014;34(27):9067–75. https://doi.org/10.1523/jneurosci.0796-14.2014.
190. Schultz A, Grouven U, Zander I, Beger FA, Siedenberg M, Schultz B. Age-related effects in the EEG during propofol anaesthesia. Acta Anaesthesiol Scand. 2004;48(1):27–34. https://doi.org/10.1111/j.1399-6576.2004.00258.x.
191. Kreuzer M, Stern MA, Hight D, et al. Spectral and entropic features are altered by age in the electroencephalogram in patients under sevoflurane anesthesia. Anesthesiology. 2020;132(5):1003–16. https://doi.org/10.1097/aln.0000000000003182.
192. Kratzer S, Schneider M, Obert DP, Schneider G, García PS, Kreuzer M. Age-related eeg features of bursting activity during anesthetic-induced burst suppression. Front Syst Neurosci. 2020;14:599962. https://doi.org/10.3389/fnsys.2020.599962.
193. Zhang X, Li A, Wang S, et al. Differences in the EEG Power spectrum and cross-frequency coupling patterns between young and elderly patients during sevoflurane anesthesia. Brain Sci. 2023. https://doi.org/10.3390/brainsci13081149.
194. Purdon PL, Pavone KJ, Akeju O, et al. The ageing brain: age-dependent changes in the electroencephalogram during propofol and sevoflurane general anaesthesia. Br J Anaesth. 2015;115:i46-57. https://doi.org/10.1093/bja/aev213.
195. Tirel O, Wodey E, Harris R, Bansard JY, Ecoffey C, Senhadji L. The impact of age on bispectral index values and EEG bispectrum during anaesthesia with desflurane and halothane in children. Br J Anaesth. 2006;96(4):480–5. https://doi.org/10.1093/bja/ael034.
196. Davidson AJ. Measuring anesthesia in children using the EEG. Paediatr Anaesth. 2006;16(4):374–87. https://doi.org/10.1111/j.1460-9592.2006.01877.x.
197. Jeleazcov C, Schmidt J, Schmitz B, Becke K, Albrecht S. EEG variables as measures of arousal during propofol anaesthesia for general surgery in children: rational selection and age dependence. Br J Anaesth. 2007;99(6):845–54. https://doi.org/10.1093/bja/aem275.
198. Sciusco A, Standing JF, Sheng Y, Raimondo P, Cinnella G, Dambrosio M. Effect of age on the performance of bispectral and entropy indices during sevoflurane pediatric anesthesia: a pharmacometric study. Paediatr Anaesth. 2017;27(4):399–408. https://doi.org/10.1111/pan.13086.
199. Obert DP, Schweizer C, Zinn S, et al. The influence of age on EEG-based anaesthesia indices. J Clin Anesth. 2021;73:110325. https://doi.org/10.1016/j.jclinane.2021.110325.
200. Kim HS, Oh AY, Kim CS, Kim SD, Seo KS, Kim JH. Correlation of bispectral index with end-tidal sevoflurane concentration and age in infants and children. Br J Anaesth. 2005;95(3):362–6. https://doi.org/10.1093/bja/aei196.
201. Ni K, Cooter M, Gupta DK, et al. Paradox of age: older patients receive higher age-adjusted minimum alveolar concentration fractions of volatile anaesthetics yet display higher bispectral index values. Br J Anaesth. 2019;123(3):288–97. https://doi.org/10.1016/j.bja.2019.05.040.
202. Hight D, Schanderhazi C, Huber M, Stüber F, Kaiser HA. Age, minimum alveolar concentration and choice of depth of sedation monitor: examining the paradox of age when using the narcotrend monitor: a secondary analysis of an observational study. Eur J Anaesthesiol. 2022;39(4):305–14. https://doi.org/10.1097/eja.0000000000001576.
203. Loison V, Voskobiynyk Y, Lindquist B, et al. Mapping general anesthesia states based on electro-encephalogram transition phases. Neuroimage. 2024;285:120498. https://doi.org/10.1016/j.neuroimage.2023.120498.
204. Schüßler J, Ostertag J, Georgii MT, et al. Preoperative characterization of baseline EEG recordings for risk stratification of post-anesthesia care unit delirium. J Clin Anesth. 2023;86:111058. https://doi.org/10.1016/j.jclinane.2023.111058.
205. Koch S, Windmann V, Chakravarty S, et al. Perioperative electroencephalogram spectral dynamics related to postoperative delirium in older patients. Anesth Analg. 2021;133(6):1598–607. https://doi.org/10.1213/ANE.0000000000005668.
206. Ostertag J, Zanner R, Schneider G, Kreuzer M. Permutation entropy does not track the electroencephalogram-related manifestations of paradoxical excitation during propofol-induced loss of

responsiveness: results from a prospective observational cohort study. Anesth Analg. 2024. https://doi.org/10.1213/ane.0000000000006919.
207. Sepúlveda P, Acosta I, Hoppe A, Lobo FA, Carrasco E. Influence of rate of administration on the mechanism behind propofol induced loss of consciousness. Rev Esp Anestesiol Reanim (Engl Ed). 2021;68(5):245–51. https://doi.org/10.1016/j.redare.2020.05.025.
208. Mehler DM, Kreuzer M, Obert DP, et al. Electroencephalographic guided propofol-remifentanil TCI anesthesia with and without dexmedetomidine in a geriatric population: electroencephalographic signatures and clinical evaluation. J Clin Monit Comput. 2024;38(4):803–15. https://doi.org/10.1007/s10877-024-01127-4.
209. Dragovic S, Schneider G, García PS, et al. Predictors of Low Risk for Delirium during Anesthesia Emergence. Anesthesiology. 2023;139(6):757–68. https://doi.org/10.1097/aln.0000000000004754.
210. Hesse S, Kreuzer M, Hight D, et al. Association of electroencephalogram trajectories during emergence from anaesthesia with delirium in the postanaesthesia care unit: an early sign of postoperative complications. Br J Anaesth. 2019;122(5):622–34. https://doi.org/10.1016/j.bja.2018.09.016.
211. Friedman D, Claassen J, Hirsch LJ. Continuous electroencephalogram monitoring in the intensive care unit. Anesth Analg. 2009;109(2):506–23. https://doi.org/10.1213/ane.0b013e3181a9d8b5.
212. Rubinos C, Alkhachroum A, Der-Nigoghossian C, Claassen J. Electroencephalogram monitoring in critical care. Semin Neurol. 2020;40(6):675–80. https://doi.org/10.1055/s-0040-1719073.
213. Vacas S, McInrue E, Gropper MA, et al. The feasibility and utility of continuous sleep monitoring in critically Ill patients using a portable electroencephalography monitor. Anesth Analg. 2016;123(1):206–12. https://doi.org/10.1213/ane.0000000000001330.
214. Carrera E, Claassen J, Oddo M, Emerson RG, Mayer SA, Hirsch LJ. Continuous electroencephalographic monitoring in critically Ill patients with central nervous system infections. Arch Neurol. 2008;65(12):1612–8. https://doi.org/10.1001/archneur.65.12.1612.
215. Vespa PM, McArthur DL, Xu Y, et al. Nonconvulsive seizures after traumatic brain injury are associated with hippocampal atrophy. Neurology. 2010;75(9):792–8. https://doi.org/10.1212/WNL.0b013e3181f07334.
216. Vespa PM, Nuwer MR, Nenov V, et al. Increased incidence and impact of nonconvulsive and convulsive seizures after traumatic brain injury as detected by continuous electroencephalographic monitoring. J Neurosurg. 1999;91(5):750–60. https://doi.org/10.3171/jns.1999.91.5.0750.
217. Ronne-Engstrom E, Winkler T. Continuous EEG monitoring in patients with traumatic brain injury reveals a high incidence of epileptiform activity. Acta Neurol Scand. 2006;114(1):47–53. https://doi.org/10.1111/j.1600-0404.2006.00652.x.
218. Katyal N, Singh I, Narula N, et al. Continuous electroencephalography (CEEG) in neurological critical care units (NCCU): a review. Clin Neurol Neurosurg. 2020;198:106145. https://doi.org/10.1016/j.clineuro.2020.106145.
219. Hilkman DM, van Mook WN, van Kranen-Mastenbroek VH. Continuous electroencephalographic-monitoring in the ICU: an overview of current strengths and future challenges. Curr Opin Anaesthesiol. 2017;30(2):192–9. https://doi.org/10.1097/aco.0000000000000443.
220. Hill CE, Blank LJ, Thibault D, et al. Continuous EEG is associated with favorable hospitalization outcomes for critically ill patients. Neurology. 2019;92(1):e9–18. https://doi.org/10.1212/wnl.0000000000006689.
221. Hofmeijer J, Beernink TM, Bosch FH, Beishuizen A, Tjepkema-Cloostermans MC, van Putten MJ. Early EEG contributes to multimodal outcome prediction of postanoxic coma. Neurology. 2015;85(2):137–43. https://doi.org/10.1212/wnl.0000000000001742.
222. Barbella G, Novy J, Marques-Vidal P, Oddo M, Rossetti AO. Prognostic role of EEG identical bursts in patients after cardiac arrest: Multimodal correlation. Resuscitation. 2020;148:140–4. https://doi.org/10.1016/j.resuscitation.2020.01.017.
223. Ruijter BJ, Tjepkema-Cloostermans MC, Tromp SC, et al. Early electroencephalography for outcome prediction of postanoxic coma: a prospective cohort study. Ann Neurol. 2019;86(2):203–14. https://doi.org/10.1002/ana.25518.
224. Amorim E, Gilmore EJ, Abend NS, et al. EEG reactivity evaluation practices for adult and pediatric hypoxic-ischemic coma prognostication in North America. J Clin Neurophysiol. 2018;35(6):510–4. https://doi.org/10.1097/wnp.0000000000000517.
225. Sheorajpanday RV, Nagels G, Weeren AJ, van Putten MJ, De Deyn PP. Quantitative EEG in ischemic stroke: correlation with functional status after 6 months. Clin Neurophysiol. 2011;122(5):874–83. https://doi.org/10.1016/j.clinph.2010.07.028.
226. Azabou E, Navarro V, Kubis N, et al. Value and mechanisms of EEG reactivity in the prognosis of patients with impaired consciousness: a systematic review. Crit Care. 2018;22(1):184. https://doi.org/10.1186/s13054-018-2104-z.
227. Claassen J, Hirsch LJ, Frontera JA, et al. Prognostic significance of continuous EEG monitoring in patients with poor-grade subarachnoid hemorrhage. Neurocrit Care. 2006;4(2):103–12. https://doi.org/10.1385/ncc:4:2:103.
228. Alkhachroum A, Appavu B, Egawa S, et al. Electroencephalogram in the intensive care unit: a focused look at acute brain injury. Intensive Care Med. 2022;48(10):1443–62. https://doi.org/10.1007/s00134-022-06854-3.
229. Williams Roberson S, Azeez NA, Fulton JN, et al. Quantitative EEG signatures of delirium and coma in mechanically ventilated ICU patients. Clin Neurophysiol. 2023;146:40–8. https://doi.org/10.1016/j.clinph.2022.11.012.
230. Andresen JM, Girard TD, Pandharipande PP, Davidson MA, Ely EW, Watson PL. Burst suppression on processed electroencephalography as a predictor of postcoma delirium in mechanically ventilated ICU patients. Crit Care Med. 2014;42(10):2244–51. https://doi.org/10.1097/ccm.0000000000000522.
231. Beuchat I, Rossetti AO, Novy J, Schindler K, Rüegg S, Alvarez V. Continuous versus routine standardized electroencephalogram for outcome prediction in critically Ill adults: analysis from a randomized trial. Crit Care Med. 2022;50(2):329–34. https://doi.org/10.1097/ccm.0000000000005311.
232. Herman ST, Abend NS, Bleck TP, et al. Consensus statement on continuous EEG in critically ill adults and children, part I: indications. J Clin Neurophysiol. 2015;32(2):87–95. https://doi.org/10.1097/wnp.0000000000000166.
233. Fogang Y, Legros B, Depondt C, Mavroudakis N, Gaspard N. Yield of repeated intermittent EEG for seizure detection in critically ill adults. Neurophysiol Clin. 2017;47(1):5–12. https://doi.org/10.1016/j.neucli.2016.09.001.
234. Hwang J, Cho SM, Ritzl EK. Recent applications of quantitative electroencephalography in adult intensive care units: a comprehensive review. J Neurol. 2022;269(12):6290–309. https://doi.org/10.1007/s00415-022-11337-y.

235. Gilmore EJ. Continuous electroencephalogram-necessity or luxury? JAMA Neurol. 2020;77(10):1211–2. https://doi.org/10.1001/jamaneurol.2020.1483.

Publisher's Note Springer Nature remains neutral with regard to jurisdictional claims in published maps and institutional affiliations.

Springer Nature or its licensor (e.g. a society or other partner) holds exclusive rights to this article under a publishing agreement with the author(s) or other rightsholder(s); author self-archiving of the accepted manuscript version of this article is solely governed by the terms of such publishing agreement and applicable law.